AFRL-IF-RS-TR-2000-149
Final Technical Report
October 2000

FOUNDATIONS OF MICROELECTROMECHANICAL SYSTEM SYNTHESIS

Carnegie Mellon University

Sponsored by
Defense Advanced Research Projects Agency
DARPA Order No. E117/0602

APPROVED FOR PUBLIC RELEASE; DISTRIBUTION UNLIMITED.

AIR FORCE RESEARCH LABORATORY
INFORMATION DIRECTORATE
ROME RESEARCH SITE
ROME, NEW YORK

This report has been reviewed by the Air Force Research Laboratory, Information Directorate, Public Affairs Office (IFOIPA) and is releasable to the National Technical Information Service (NTIS). At NTIS it will be releasable to the general public, including foreign nations.

AFRL-IF-RS-TR-2000-149 has been reviewed and is approved for publication.

APPROVED:

ROBERT G. HILLMAN
Project Engineer

FOR THE DIRECTOR:

NORTHRUP FOWLER, Technical Advisor
Information Technology Division
Information Directorate

If your address has changed or if you wish to be removed from the Air Force Research Laboratory Rome Research Site mailing list, or if the addressee is no longer employed by your organization, please notify AFRL/IFTC, 26 Electronic Pky, Rome, NY 13441-4514. This will assist us in maintaining a current mailing list.

Do not return copies of this report unless contractual obligations or notices on a specific document require that it be returned.

FOUNDATIONS OF MICROELECTROMECHANICAL SYSTEM SYNTHESIS

Gary K. Fedder

Contractor: Carnegie Mellon University
Contract Number: F30602-96-2-0304
Effective Date of Contract: 26 August 1996
Contract Expiration Date: 31 December 1999
Short Title of Work: Foundation of Microelectro-mechanical System Synthesis
Period of Work Covered: Aug 96 - Dec 99

Principal Investigator: Gary K. Fedder
Phone: (412) 268-8443
AFRL Project Engineer: Robert G. Hillman
Phone: (315) 330-4961

This research was supported by the Defense Advanced Research Projects Agency of the Department of Defense and was monitored by Robert G. Hillman, AFRL/IFTC, 26 Electronic Pky, Rome, NY.

REPORT DOCUMENTATION PAGE	Form Approved OMB No. 0704-0188

1. AGENCY USE ONLY *(Leave blank)*	2. REPORT DATE	3. REPORT TYPE AND DATES COVERED
	OCTOBER 2000	Final Aug 96 - Dec 99

4. TITLE AND SUBTITLE
FOUNDATIONS OF MICROELECTROMECHANICAL SYSTEM SYNTHESIS

5. FUNDING NUMBERS
C - F30602-96-2-0304
PE - 63739E
PR - E117
TA - 00
WU - 00

6. AUTHOR(S)
Gary K. Fedder

7. PERFORMING ORGANIZATION NAME(S) AND ADDRESS(ES)
Carnegie Mellon University
Office of Sponsored Research
500 Forbes Ave
PO Box 371032M
Pittsburg PA 15213-3890

8. PERFORMING ORGANIZATION REPORT NUMBER
N/A

9. SPONSORING/MONITORING AGENCY NAME(S) AND ADDRESS(ES)
Defense Advanced Research Projects Agency
3701 N. Fairfax Drive
Arlington VA 22060-6218

Air Force Research Laboratory/IFTC
26 Electronic Pky
Rome New York 13441-4514

10. SPONSORING/MONITORING AGENCY REPORT NUMBER
AFRL-IF-RS-TR-2000-149

11. SUPPLEMENTARY NOTES
Air Force Research Laboratory Project Engineer: Robert G. Hillman/IFTC/(315) 330-4961

12a. DISTRIBUTION AVAILABILITY STATEMENT
APPROVED FOR PUBLIC RELEASE; DISTRIBUTION UNLIMITED.

12b. DISTRIBUTION CODE

13. ABSTRACT *(Maximum 200 words)*

In this survey paper we describe and contrast three different approaches for extending circuit simulation to include micromachined devices. The most commonly used method, that of using physical insight to develop parameterized macromodels, is presented first. The issues associated with fitting the parameters to simulation data while incorporating design attribute dependencies is considered. The numerical model order reduction approach to macromodeling is presented second, and some of the issues associated with fast solvers and model reduction are summarized. Lastly, we describe the recently developed circuit-based approach for simulating micromachined devices, and describe the design hierarchy and the use of a catalog of parts.

14. SUBJECT TERMS
MEMS, Synthesis, Resonators, EDA

15. NUMBER OF PAGES
56

16. PRICE CODE

17. SECURITY CLASSIFICATION OF REPORT	18. SECURITY CLASSIFICATION OF THIS PAGE	19. SECURITY CLASSIFICATION OF ABSTRACT	20. LIMITATION OF ABSTRACT
UNCLASSIFIED	UNCLASSIFIED	UNCLASSIFIED	UL

Table of Contents

List of Figures

1. Project Summary

Project Goal

The two primary objectives of the "Foundations for MEMS Synthesis" project were to develop:

- A VLSI-like Hierarchy for MEMS
- MEMS Synthesis Flow

Our technical approach comprised four major tasks that focus on the circuit-level design of MEMS. The tasks are partitioned by placement in the synthesis flow: structural synthesis, circuit/layout synthesis, shape and process optimization, hierarchical representation and performance verification, and technology integration and transfer. Figure 1 illustrates the relationship between these research areas. Each of the participating investigators in the tasks developed prototypical implementations of point design tools that fit within the synthesis-centric MEMS design methodology. Across all the tasks, these implementations support the overall design flow through use of a common hierarchical representation of MEMS and use of a common set of components.

When the project began, the primary design representations for MEMS were layout and 3D solid modeling with customized meshes for each finite/boundary element simulator. The choice of the layout representation was itself a challenge.

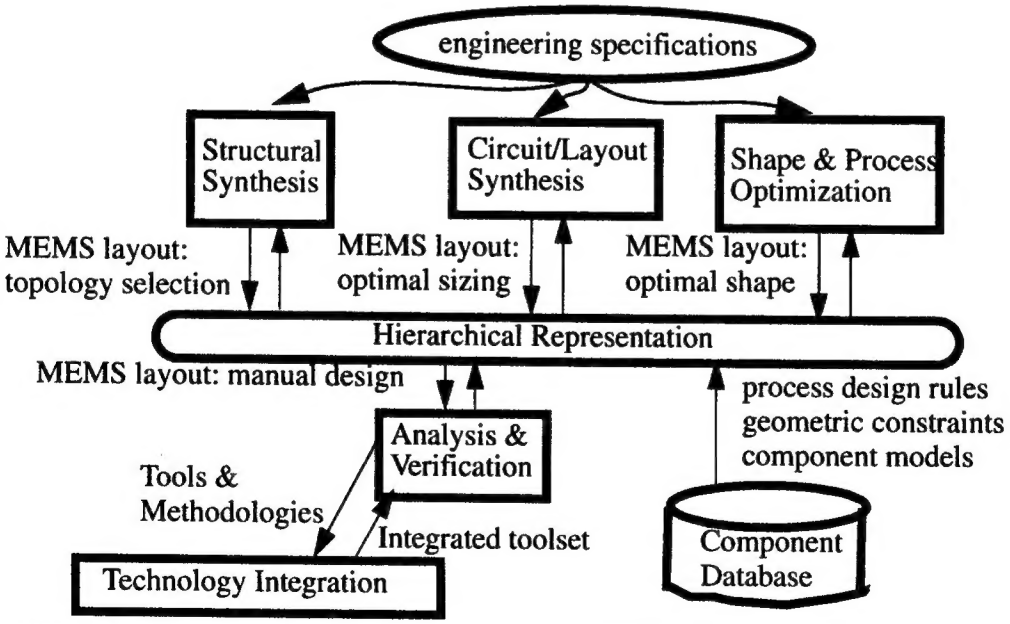

FIGURE 1. Relationship between project tasks for the MEMS synthesis flow.

from the commonplace layout representation to a schematic representation. However, the list of elements in the component database remained the same. This project has therefore participated in two revolutions in design representations for MEMS during the course of the project.

Development in this project of the behavioral simulation environments at Carnegie Mellon and U.C. Berkeley have enabled a revolution in the design representation. Specifically, the introduction of the design representation abstractions at the *schematic* and layout level instead of the 3D solid model or mesh level addresses the first of the two primary goals of this project. These levels of abstractions now enable a MEMS designer to iteratively design a complete MEMS sensor or actuator system, instead of just a focused portion of the transducer element.

The second goal of the project, a synthesis-based design flow, allows expert MEMS designers to capture and encode design constraints and enables novice MEMS designers to develop MEMS designs that have a higher chance of working during the first pass at fabrication. During the project we demonstrated both the individual tools in this flow, as well as some interactions between the tools.

The impact of these new levels of abstraction and the new design methodology is the ability of the designer to *directly* link the impact of MEMS device level innovations with quality improvements in the final *system* design as well as enable the top-down design of MEMS [1][13][14][25][29][33].

2. Capabilities Developed During the Project

The set of capabilities developed during the project to support the hierarchical design representation and synthesis flow are detailed for each task. A tutorial summary of much of this work will be published in *IEEE Transactions on CAD* [38]. A draft preprint of this paper is attached to the report.

Task 1: Structural Synthesis (CMU)

Structural synthesis involves choosing a design topology that meets the required engineering specifications for the MEMS device. In this project we developed a shape-grammar based topology representation for MEMS [20][22][30], an A-Design based search algorithm to choose amongst competing topologies [16][21], and a hierarchical method for rapid evaluation of the performance of candidate design topologies. The resulting integration of these three concepts were used to demonstrate a methodology to configure new resonator and accelerometer structures automatically.

FIGURE 2. Structural Synthesis using A-Design proposes MEMS topologies that transform the user specified input functional domain into the user specified output functional domain.

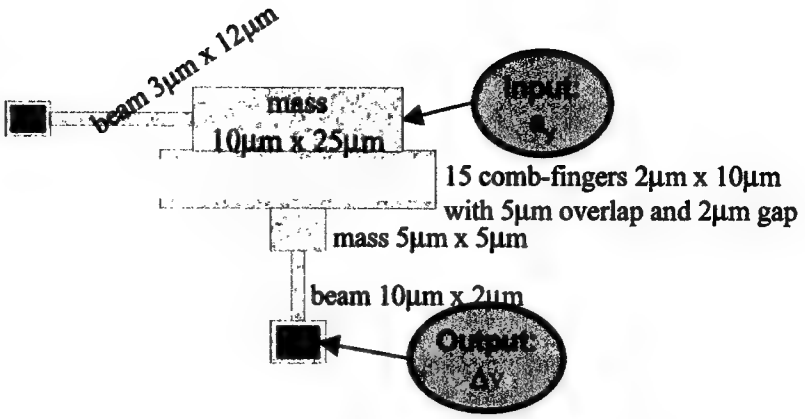

By representing the desired input and output energy domains, and using a component database that provides elements that can translate between various energy domains, the A-Design based search algorithm identifies candidate topologies that meet the designers requirements. The use of a shape-grammar for topology representation leads to the encoding of the MEMS layout (i.e., shape), allowing the search algorithm to directly interface with the common hierarchical representation for the synthesis-centric design flow. The hierarchical evaluation method is based on behavioral simulation environments detailed in Task 4, and allows the A-design search engine to have a range of performance evaluators ranging from fast with less accuracy (for the early stages of A-design) to slow and accurate (for the final iterations in A-design). The example in Figure 2 shows acceleration input and voltage output respectively and shows that the structural synthesis methodology led to topologies that are different from conventional manual design.

Task 2: Circuit/Layout Synthesis (CMU)

The circuit/layout synthesis algorithms developed during this project can be employed to optimally size a fixed topology to meet the user specified engineering performance parameters. The fixed topology could be generated by the automated methodology in Task 1 or through manual design. Three topology-specific synthesis modules were developed in this task: a folded-flexure resonator in the MUMPS process [2][11][23][37], a lateral accelerometer in the MUMPS process [26][27], as well as an accelerometer in the CMOS-MEMS process [36]. The CMOS-MEMS accelerometer ties into the joint DARPA MTO MEMS and Composite CAD funded project on "Integrated MEMS Inertial Measurement Unit." These synthesis modules are based on lumped parameter models that map the design parameters defining the layout geometry into the design per-

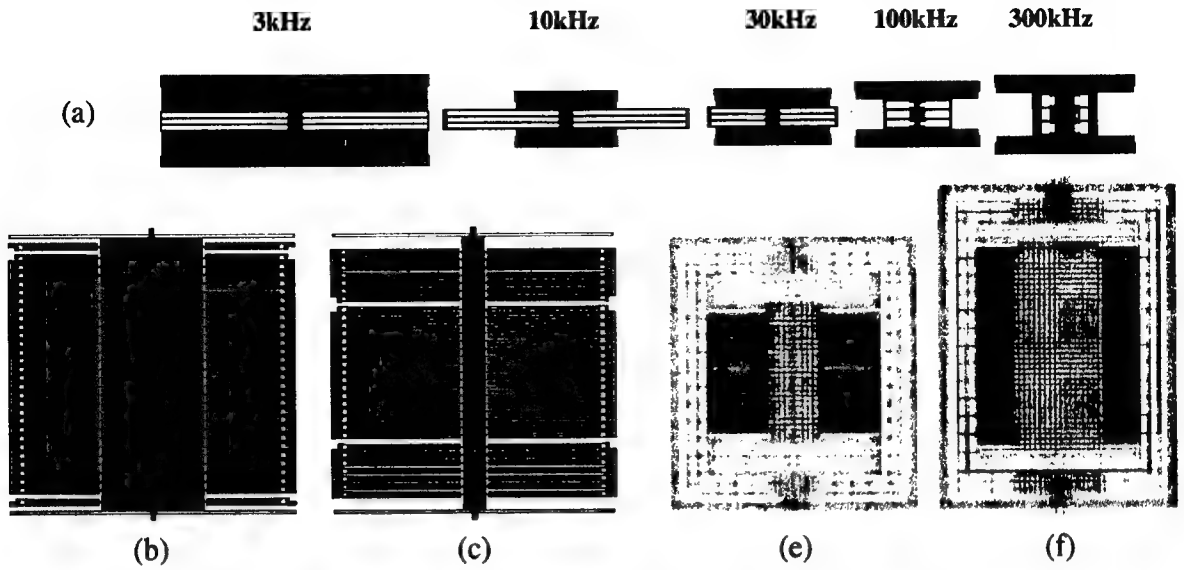

FIGURE 3. Synthesized layouts of (a) family of resonators optimized for area, voltage and thickness; MUMPS accelerometers under (b) open-loop and (c) closed-loop operation optimized range; and (e) CMOS-MEMS accelerometers compared to (f) manual design.

formance space, and generate an optimization-based layout. These models incorporate manufacturing variations, such as those affecting cross-axis sensitivity in accelerometers, as well as the capacitive load and noise parameters of the circuits that condition the signal output from the MEMS sensor. Example synthesized layouts from each of the modules are shown in Figure 3.

We have demonstrated that such synthesis modules enable designers of integrated MEMS to synthesize layouts that meet their design needs on demand. These modules demonstrate the crucial MEMS design trade-offs for a specific application to novice MEMS designers. Cronos Integrated Microsystems is using a web-based interface to these synthesis tools in their short course on MEMS. Microcosm Technologies, Inc. is licensing the technology developed during this task with plans for offering it as a teaching aid. The topology specificity of the synthesis modules and the current lack of automation in macromodel generation prevents a more general tool at this time.

To overcome this limitation, progress has been made to integrate the optimization framework developed in Task 2 with the behavioral simulation methodology in Task 4. This integration will allow any user comfortable with the simulation methodology to use the circuit/layout synthesis technologies for automated design. Additionally, we fabricated four optimized CMOS-MEMS accelerometers to experimentally verify the models in the synthesis module (previous experimental fabrication of MUMPS resonators showed that the models compared to within 10% of the fabricated devices). Testing of these devices will occur under another DARPA-MTO project.

Task 3: Shape and Process Optimizations (MIT, UPenn)

The MIT efforts focused on developing fast algorithms for computing sensitivities in numerical simulation, to provide search directions for the shape optimization efforts at UPenn, as well as for developing a framework for process optimization. Fast computations for electrostatic sensitivities were demonstrated in the first year [6], and a rigid elastic formulation coupled with multi-level Newton solution subsequently demonstrated additional speedups [9]. Optimization algorithms for obtaining the shape of compliant structures to meet the desired force-deflection characteristics were demonstrated at UPenn [17][19]. As an extension of the static force-deflection problem, the structural synthesis for dynamic specifications such as the (eigen) modeshapes of a ring gyroscope were demonstrated [18]. The third subtask on process optimization frameworks, at MIT, led to the development of process representation and repository methods for capturing manufacturing variation (implemented using the "Semiconductor Process Representation" standard); propagation of process variation to structure variation; and analysis of process variation on device performance. This task was linked with the rest of the project in several ways: one of the static force-deflection examples at UPenn involved the maximizing the mechanical displacement of an inertial mass using a compliant mechanism to link with the accelerometer synthesis efforts in Task 2. Also, the resonator synthesis module of Task 2 was modified to link with the process variation framework developed in Task 3 to trade-off between resonator area and frequency variation.

Task 4: Hierarchical Representation and Performance Verification (CMU, UC Berkeley)

The Carnegie Mellon and UC Berkeley efforts independently demonstrated the concept of composing MEMS devices from a library of parameterized behavioral models. Additionally, through the gyroscope canonical problem, a multi-level hierarchical design methodology was demonstrated. The tools developed in this sub-task have created a powerful new schematic design-entry mode for MEMS as an alternative to solid-modeling and layout.

By developing an initial hierarchical representation, and a library catalog of "atomic" elements found in suspended MEMS, and subsequently developing behavioral models of these elements, the performance verification of resonators [8], accelerometers [10], vibratory rate gyroscopes [7], and micropositioners [35] were demonstrated. Subsequent improvements in the hierarchical representation simplified the user interface between the designer and the simulation environment, and also led to a speed-up in simulation times. Additional improvements in the elemental behavioral models, and in models of higher level elements (such as the comb-drive) led to

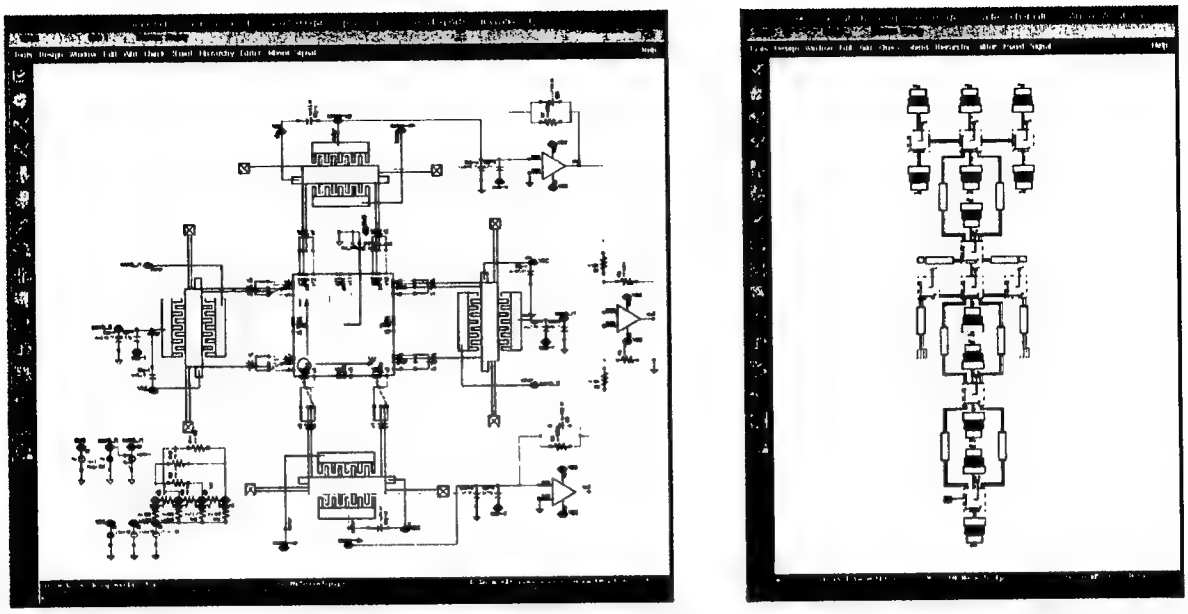

FIGURE 4. (a) High level NODAS schematic of canonical gyroscope consisting of four spring and comb sections a plate mass and several circuits, with a (b) hierarchical lower-level schematic of one of the 4 spring and comb sections.

improved simulation accuracy as well as simulation performance. The current Cadence-based Carnegie Mellon tool (NODAS) [8][10][24][28][31][32][34] and MATLAB-based UC Berkeley tool (SUGAR) [12][15] represent the second-generation schematic-based design tools for MEMS. As shown in Figure 4(b), the atomic elements include beams, plates, comb-drives, and anchors, which can be combined to form higher-level schematics as in Figure 4(a). The ability to link elements from the catalog at multiple levels of the design hierarchy through a common representation enables mixed-level simulation of MEMS.

Task 5: Technology Integration and Transfer (Microcosm)

The tools and methodologies developed in this project were transferred to Microcosm during annual workshops held at Microcosm. The first year workshop ran though the entire summer allowing close student interaction [3][4][5] and choice of interfaces between the student-level tasks. Subsequent workshops ran for a single week and provided students with an intensive environment for demonstrating their latest developments, as well as integrating between selected development activities. Microcosm has licensed the fast sensitivity computation developed at MIT, and is licensing the NODAS schematic representation and behavioral models and the synthesis modules from Carnegie Mellon. NODAS will be packaged with Microcosm's MEMSYS system-level design environment,

and will complement their existing macromodel generation features.

3. Deliverable Checklist

- Q4-97: 2D microresonator synthesis module (CMU)
- Q4-97: Semiconductor process representation with statistical extensions & MUMPS implementation
- Q1-98: 3D microresonator synthesis module (CMU)
- Q1-98: First-generation MEMS MAST library - NODAS 1.0 (CMU)
- Q1-98: DC/steady-state simulation of 2D beam/gap systems in MATLAB - Sugar 0.4 (UCB)
- Q1-98: MEMCAD 4.0 (improved macromodeling technology for use in MEMSYN efforts) (MIT/Microcosm)
- Q2-98: 2D shape synthesis for specified force-deflection behavior (U. Penn)
- Q3-98: Transient analysis planar beam/gap systems in MATLAB - Sugar (UCB)
- Q3-98: Nonlinear beam modeling in MATLAB - Sugar (UCB)
- Q1-99: Fast geometric sensitivity computation (MIT)
- Q1-99: MEMCAD 4.5 (insertion of MEMS schematic technology) (Microcosm/CMU)
- Q1-99: Simulation of nonlinear 3D beam/gap systems - Sugar (UCB)
- Q2-99: Microaccelerometer synthesis module (CMU)
- Q2-99: Second-generation analog-HDL schematic library (CMU)
- Q3-99: Layout-based schematic library (CMU)
- Q3-99: Shape optimization of a non-linear mechanical structure (U. Penn)
- Q4-99: CMOS-MEMS microaccelerometer synthesis module (CMU)

4. Publications

[1] T. Mukherjee and G. K. Fedder, "Structured Design of Microelectromechanical Systems," in *Proceedings of the 34th Design Automation Conference*, Anaheim, CA, June 9-13, 1997, pp. 680-685.

[2] G. K. Fedder, S. Iyer, and T. Mukherjee, "Automated Optimal Synthesis of Microresonators," in *Technical Digest of the IEEE Intl. Conf. on Solid-State Sensors and Actuators (Transducers '97)*, Chicago, IL, June 16-19, 1997, v. 2, pp. 1109-1112.

[3] Michael S.-C. Lu, "The modeling and control system design for an electrostatic micro-actuator", Aug 1997.

[4] Elizabeth K. Lai, "Modeling of a Micromachined Vibrating Ring Gyroscope Using MEMCAD and Simulink", Aug 1997.

[5] Michael D. Pottenger, "System Simulation of Micromachined Differential Capacitive Inertial Sensors", Aug 1997.

[6] J. Wang and J. White, "Fast Algorithms for Computing Electrostatic Geometric Sensitivities," *Intl. Conf. on Simulation of Semiconductor Processes and Devices (SISPAD)*, Boston, September, 1997, pp. 121-124.

[7] M. S. Kranz and G. K. Fedder, "Micromechanical Vibratory Rate Gyroscopes Fabricated in Conventional CMOS," *Symposium Gyro Technology*, Stuttgart, Germany, Sept. 1997.

[8] J. E. Vandemeer, M. S. Kranz, and G. K. Fedder, "Nodal Simulation of Suspended MEMS with Multiple Degrees of Freedom," *Proc. 1997 International Mechanical Engineering Congress and Exposition: The Winter Annual Meeting of ASME in the 8th Symposium on Microelectrome-*

chanical Systems, Dallas, TX, Nov. 16-21, 1997

[9] N. R. Aluru and J. White, "A Fast Integral Equation Technique for Analysis of Microflow Sensors Based on Drag Force Calculations," *Proc. 1998 Int. Conf. on Modeling and Simulation of Microsystems, Semiconductors, Sensors and Actuators (MSM '98)*, Santa Clara, CA, April 6-8, 1998.

[10]J. E. Vandemeer, M. S. Kranz, G. K. Fedder, "Hierarchical Representation and Simulation of Micromachined Inertial Sensors," *Proc. 1998 Int. Conf. on Modeling and Simulation of Microsystems, Semiconductors, Sensors and Actuators (MSM '98)*, Santa Clara, CA, April 6-8, 1998.

[11]S. Iyer, T. Mukherjee, and G. K. Fedder, "Multi-Mode Sensitive Layout Synthesis of Microresonators," *Proc. 1998 Int. Conf. on Modeling and Simulation of Microsystems, Semiconductors, Sensors and Actuators (MSM '98)*, Santa Clara, CA, April 6-8, 1998.

[12]J. Clark, N. Zhou, S. Brown, and K.S.J.Pister, "Nodal Analysis for MEMS Simulation and Design," *Proc. 1998 Int. Conf. on Modeling and Simulation of Microsystems, Semiconductors, Sensors and Actuators (MSM '98)*, Santa Clara, CA, April 6-8, 1998.

[13]T. Mukherjee and G. K. Fedder, "Design Methodology for Mixed Domain Systems on a Chip," *Proc. IEEE Computer Society Workshop on VLSI*, Orlando, FL, April 16-17, 1998.

[14]R. D. Blanton, G. K. Fedder, and T. Mukherjee, "Hierarchical Design and Test of MEMS," *Microsystems Technology News*, April 1998.

[15]J. Clark, N. Zhou, S. Brown, and K.S.J.Pister, "Fast, accurate MEMS simulation with SUGAR 0.4," in *Proc. of the Sensors and Actuator Workshop*, Hilton Head Is., SC, June 1998.

[16]M. Campbell, J. Cagan, and K. Kotovsky, "A-Design: Theory and Implementation of and Adaptive, Agent-Based Method of Conceptual Design," *Artificial Intelligence in Design '98*, Lisbon, July 20-23, 1998.

[17]A. Saxena and G. K. Ananthasuresh, "Topology Synthesis of Compliant Mechanisms Using the Optimality Criteria Method," *Proc. of the AIAA/USAF/NASA/ISSMO 1998 Symposium on Multi-disciplinary Analysis and Optimization*, Vol. 3, pp. 1990-1910, St. Louis, MO, Sept. 2-4, 1998.

[18]E. Lai and G. K. Ananthasuresh, "An Optimization Approach to the Design for Desired Mode Shapes: Preliminary Results," *Proc. of the 1998 ASME Biennial Mechanisms Conference,* Atlanta, GA, Paper # DETC/DAC-5632, Sept. 14-16 1998.

[19]A. Saxena and G.K. Ananthasuresh, "An Optimality Criteria Approach for the Topology Synthesis of Compliant Mechanisms," *Proc. of the 1998 ASME Biennial Mechanisms Conference*, Atlanta, GA, Paper # DETC/MECH-5937, Sept. 14-16 1998.

[20]M. Agarwal and J. Cagan, "Robust Activity Analysis -- Partitioning Non-Monotonic Design Spaces into Robust Optimal Regions," *Proceedings of the 1998 ASME Design Engineering Technical Conferences and Computers in Engineering Conference: Design Automation Conference,* DETC98/DAC-6012, Atlanta, GA, September 13-16, 1998.

[21]M. Campbell, J. Cagan and K. Kotovsky, "Agent-based Synthesis of Electro-Mechanical Design Configurations," *Proceedings of the 1998 ASME Design Engineering Technical Conferences and Computers in Engineering Conference: Design Theory and Methodology Conference,* DETC98/DTM-, Atlanta, GA, September 13-16, 1998. [Winner - Xerox Best Paper Award]

[22]K. G. Constantine, M. Agarwal, and J. Cagan, "Product Design Generation and Manufacturing Cost Evaluation Through Shape Grammars", *The Third International Conference on Integrated Design and Process Technology*, Berlin.

[23]T. Mukherjee, S. Iyer, and G. K. Fedder, "Optimization-based synthesis of microresonators," *Sensors and Actuators A*, 70 (1998), pp 118-127.

[24]G. K Fedder an Q. Jing, "NODAS 1.3 - Nodal Design Of Actuators And Sensors," in *Proc. of IEEE/VIUF Int. Workshop on Behavioral Modeling and Simulation*, Orlando, FL, October 27-28, 1998.

[25]G. Fedder, "Structured design for Integrated MEMS," *IEEE MEMS '99*, Orlando, FL, January 17-21, 1999.

[26]T. Mukherjee, Y. Zhou, and G. K. Fedder, "Automated optimal synthesis of microaccelerometers," *IEEE MEMS '99*, Orlando, FL, January 17-21, 1999.

[27]\S. Iyer, Y. Zhou and T. Mukherjee, "Analytical Modeling of Cross-axis Coupling in Micromechanical Springs", *Proc. 1999 Int. Conf. on Modeling and Simulation of Microsystems, Semiconductors, Sensors and Actuators (MSM '99)*, Puerto Rico, April 19-21, 1999, pp. 632-635.

[28]Michael S.-C. Lu and Gary K. Fedder, "Parameterized Electrostatic Gap Models for Structured Design of Microelectromechanical Systems", *Proc. 1999 Int. Conf. on Modeling and Simulation of Microsystems, Semiconductors, Sensors and Actuators (MSM '99)*, Puerto Rico, April 19-21, 1999, pp. 280-283.

[29]T. Mukherjee and G. K. Fedder, "Hierarchical Mixed-Domain Circuit Simulation, Synthesis and Extraction Methodology for MEMS," *Kluwer Journal of VLSI Signal Processing on System Design*, vol. 21, no. 3, pp. 233-249, July 1999.

[30]M. Agarwal and J. Cagan, "Systematic form and function design of MEMS resonators using shape grammars," *Int. Conf. on Engineering Design (ICED 99)*, Munich, Germany, August 24-26, 1999.

[31]Q. Jing, T. Mukherjee and G. K. Fedder, "A Design Methodology for Micromechanical Bandpass Filters," *Proc. IEEE Behavioral Modeling And Simulation Workshop*, Oct. 6, 1999.

[32]G. K. Fedder and Q. Jing, "A Hierarchical Circuit-Level Design Methodology for Microelectromechanical Systems," *IEEE Trans. on Circuits and Systems II: Analog and Digital Signal Processing*, v. 46, n. 10, October 1999, pp. 1309-1315.

[33]T. Mukherjee, G. K. Fedder and R. D. Blanton, "Hierarchical Design and Test of Integrated Microsystems," *IEEE Design and Test*, v.16, n.4, October-December 1999, pp. 18-27.

[34]Q. Jing, T. Mukherjee and G. K. Fedder, "CMOS Micromechanical Bandpass FIlter Design Using a Hierarchical MEMS Circuit Library," to appear in *IEEE Microelectromechanical Systems Conference*, Miyazaki, Japan, January 23-27, 2000

[35]H. Xie, L. Erdmann, Q. Jing, G.K. Fedder, "Simulation and characterization of a CMOS z-axis microactuator with electrostatic comb drives", to be presented at *2000 Int. Conf. on Modeling and Simulation of Microsystems, Semiconductors, Sensors and Actuators (MSM '00)*, San Diego, CA; 27-29 Mar. 2000.

[36]V. Gupta and T. Mukherjee, "Layout Synthesis of CMOS MEMS Accelerometers," to be presented at *2000 Int. Conf. on Modeling and Simulation of Microsystems, Semiconductors, Sensors and Actuators (MSM '00)*, San Diego, CA; 27-29 Mar. 2000.

[37]N. Deb, S. Iyer, T. Mukherjee and R. D. Blanton, "MEMS Resonator Synthesis for Defect Reduction," to appear in *Journal of Modeling and Simulation of MEMS*.

[38]T. Mukherjee, G. K. Fedder, and J. White, "Emerging Simulation Approaches for Micromachined Devices," submitted for publication in *IEEE Trans. on CAD*, June 2000.

5. Presentations

[1] T. Mukherjee, "Foundations for MEMS Synthesis," *MCNC MUMPS Users Group Meeting*, Nov. 8, 1996.

[2] T. Mukherjee, "Structured Design of Microelectromechanical Systems," in *34th Design Auto-*

mation Conference, Anaheim, CA, June 9-13, 1997.
[3] G. K. Fedder, "Automated Optimal Synthesis of Microresonators," in *IEEE Intl. Conf. on Solid-State Sensors and Actuators (Transducers '97)*, Chicago, IL, June 16-19, 1997.
[4] G.K. Ananthasuresh, "Sensitivity Calculations for Designing with Flexibility," Center for Computational Design, Rutgers University, New Brunswick, NJ, July 17, 1997.
[5] ,D. Boning, "Distributed Design of Semiconductor Processes," MIT/Stanford DARPA Demonstration, MIT, Cambridge, MA, September 9, 1997.
[6] M. S. Kranz, "Micromechanical Vibratory Rate Gyroscopes Fabricated in Conventional CMOS," *Symposium Gyro Technology*, Stuttgart, Germany, Sept. 1997.
[7] K. Pister, "CAD for MEMS," presented at UC Berkeley - MEMS Seminar, September 1997.
[8] J. Wang, "Fast Algorithms for Computing Electrostatic Geometric Sensitivities," International Conference on Simulation of Semiconductor Processes and Devices, Cambridge, MA, Sept., 1997.
[9] J. E. Vandemeer, "Nodal Simulation of Suspended MEMS with Multiple Degrees of Freedom," *1997 International Mechanical Engineering Congress and Exposition: The Winter Annual Meeting of ASME in the 8th Symposium on Microelectromechanical Systems*, Dallas, TX, Nov. 16-21, 1997.
[10]G. K. Fedder, "Design and Fabrication of CMOS-Based Microelectromechanical Systems," Mechanical Engineering Departmental Seminar, University of Pittsburgh, Pittsburgh, PA, November 14, 1997. (invited)
[11]G. K. Fedder, "CMOS-Based MEMS Sensors," BSAC Seminar, University of California at Berkeley, Berkeley, CA, December 19, 1997.
[12]N. R. Aluru, "A Fast Integral Equation Technique for Analysis of Microflow Sensors Based on Drag Force Calculations," *1998 Int. Conf. on Modeling and Simulation of Microsystems, Semiconductors, Sensors and Actuators (MSM '98)*, Santa Clara, CA, April 6-8, 1998.
[13]J. E. Vandemeer, "Hierarchical Representation and Simulation of Micromachined Inertial Sensors," *1998 Int. Conf. on Modeling and Simulation of Microsystems, Semiconductors, Sensors and Actuators (MSM '98)*, Santa Clara, CA, April 6-8, 1998.
[14]S. Iyer, "Multi-Mode Sensitive Layout Synthesis of Microresonators," *1998 Int. Conf. on Modeling and Simulation of Microsystems, Semiconductors, Sensors and Actuators (MSM '98)*, Santa Clara, CA, April 6-8, 1998.
[15]N. Zhou, "Nodal Analysis for MEMS Simulation and Design," *1998 Int. Conf. on Modeling and Simulation of Microsystems, Semiconductors, Sensors and Actuators (MSM '98)*, Santa Clara, CA, April 6-8, 1998.
[16]T. Mukherjee, "Design Methodology for Mixed Domain Systems on a Chip," *IEEE Computer Society Workshop on VLSI*, Orlando, FL, April 16-17, 1998.
[17]G.K. Ananthasuresh, "Topology and Shape Design Using Optimization Techniques," A talk given to the MEMS group at the Sandia National Laboratories, Albuquerque, NM, June 15th, 1998.
[18]J. Clark, "Fast, accurate MEMS simulation with SUGAR 0.4," *Sensors and Actuator Workshop*, Hilton Head Is., SC, June 1998.
[19]M. Campbell, "A-Design: Theory and Implementation of and Adaptive, Agent-Based Method of Conceptual Design," *Artificial Intelligence in Design '98*, Lisbon, July 20-23, 1998.
[20]G. K. Ananthasuresh, "Shape Optimization of Structures for Desired Mode Shapes," Delphi Automotive Systems, Kokomo, IN, August 29, 1998. Hosts: Dr. James Logsdon and Mr. George Qiang.

[21]A. Saxena, "Topology Synthesis of Compliant Mechanisms Using the Optimality Criteria Method," *Proc. of the AIAA/USAF/NASA/ISSMO 1998 Symposium on Multi-disciplinary Analysis and Optimization*, St. Louis, MO, Sept. 2-4, 1998.

[22]E. Lai, "An Optimization Approach to the Design for Desired Mode Shapes: Preliminary Results," *1998 ASME Biennial Mechanisms Conference,* Atlanta, GA, Sept. 14-16 1998.

[23]A. Saxena, "An Optimality Criteria Approach for the Topology Synthesis of Compliant Mechanisms," *1998 ASME Biennial Mechanisms Conference*, Atlanta, GA, Sept. 14-16 1998.

[24] M. Agarwal, "Robust Activity Analysis -- Partitioning Non-Monotonic Design Spaces into Robust Optimal Regions," *1998 ASME Design Engineering Technical Conferences and Computers in Engineering Conference: Design Automation Conference*, Atlanta, GA, September 13-16, 1998.

[25]M. Campbell, "Agent-based Synthesis of Electro-Mechanical Design Configurations," *Proceedings of the 1998 ASME Design Engineering Technical Conferences and Computers in Engineering Conference: Design Theory and Methodology Conference,* Atlanta, GA, September 13-16, 1998. [Winner - Xerox Best Paper Award]

[26]K. G. Constantine, "Product Design Generation and Manufacturing Cost Evaluation Through Shape Grammars", *The Third International Conference on Integrated Design and Process Technology*, Berlin.

[27]G. K Fedder, "NODAS 1.3 - Nodal Design Of Actuators And Sensors," in *Proc. of IEEE/VIUF Int. Workshop on Behavioral Modeling and Simulation*, Orlando, FL, October 27-28, 1998.

[28]G. Fedder, "Structured design for Integrated MEMS," *IEEE MEMS '99*, Orlando, FL, January 17-21, 1999.

[29]T. Mukherjee, "Automated optimal synthesis of microaccelerometers," *IEEE MEMS '99*, Orlando, FL, January 17-21, 1999.

[30]S. Iyer, "Analytical Modeling of Cross-axis Coupling in Micromechanical Springs", *1999 Int. Conf. on Modeling and Simulation of Microsystems, Semiconductors, Sensors and Actuators (MSM '99)*, Puerto Rico, April 19-21, 1999.

[31]Michael S.-C. Lu, "Parameterized Electrostatic Gap Models for Structured Design of Microelectromechanical Systems", *1999 Int. Conf. on Modeling and Simulation of Microsystems, Semiconductors, Sensors and Actuators (MSM '99)*, Puerto Rico, April 19-21, 1999.

[32]M. Agarwal, "Systematic form and function design of MEMS resonators using shape grammars," *Int. Conf. on Engineering Design (ICED 99)*, Munich, Germany, August 24-26, 1999.

[33]G. K. Fedder, "Characterization and Reliability of CMOS Microstructures," *SPIE Symposium on Micromachining and Microfabrication*, Sept. 1999.

[34]Q. Jing, "A Design Methodology for Micromechanical Bandpass Filters," *Proc. IEEE Behavioral Modeling And Simulation Workshop*, Oct. 6, 1999.

6. Theses

[1] J. Wang, "The Geometric Sensitivity Analysis of Electrostatic Field for Microelectromechanical System Simulation," Thesis, Master of Science, MIT, Boston, MA, June, 1997.

[2] M. Agarwal, "A Language of Coffee Makers," Thesis, Master of Science, Carnegie Mellon, Pittsburgh, PA, May, 1997.

[3] Matthew Campbell, "A-Design: An Agent-Based Conceptual Design Methodology," Thesis, Master of Science, Carnegie Mellon, Pittsburgh, PA, May, 1997.

[4] J. E. Vandemeer, "Nodal Design of Actuators and Sensors (NODAS)," Master of Science, Carnegie Mellon, Pittsburgh, PA, May 1998.

[5] M. S. Kranz, "Design and Simulation of Two Novel Micromechanical Gyroscopes," Master of Science, Carnegie Mellon, Pittsburgh, PA, May 1998.
[6] S. Iyer, "Layout Synthesis of Microresonators," Master of Science, Carnegie Mellon, Pittsburgh, PA, May 1998.
[7] Y. Zhou, "Layout Synthesis of Microaccelerometers," Master of Science, Carnegie Mellon, Pittsburgh, PA, September 1998.

7. Technology Transfer Plans

Microcosm Technologies has licensed some of the tools and methodologies developed in this project. MEMSCAP has expressed interest in licensing some of these tools and methodologies. In particular, the NODAS schematic representation, as well as the schematic-centric design environment it has spawned will be included in MEMSCAP's Kanaga design kit for MUMPS and in a yet to be developed CMOS-MEMS design kit for the DARPA MTO MEMS project on "Application-Specific Integrated-MEMS Process Service."

8. Future Extensions

To address the link between the schematic and layout representations, a layout to schematic extractor is being developed under the joint DARPA MTO MEMS and Composite CAD project on "Integrated MEMS Inertial Measurement Unit," and schematic-driven layout generation is being developed under the DARPA MTO MEMS project on "Application-Specific Integrated MEMS Process Service."

Extensions of the hierarchical representation methodology to enable layout generation and design rule checking is being developed under the auspices of the DARPA MTO "Application-Specific Integrated MEMS Process Service" project, and MEMS and parasitic extraction is being developed in the DARPA MTO "Integrated MEMS Inertial Measurement Unit" project. These efforts link the schematic representation developed in this project with the existing layout and solid model representations allowing the MEMS designer to choose their preferred mode of design entry and design simulation independently.

Appendix

Emerging Simulation Approaches For Micromachined Devices

T. Mukherjee and G. Fedder
Department of Electrical and Computer Engineering
Carnegie Mellon University
Pittsburgh, PA 15213-3890
J. White
Department of Electrical Engineering and Computer Science,
Research Laboratory of Electronics,
Massachusetts Institute of Technology
Cambridge, MA. 02139

ABSTRACT

In this survey paper we describe and contrast three different approaches for extending circuit simulation to include micromachined devices. The most commonly used method, that of using physical insight to develop parameterized macromodels, is presented first. The issues associated with fitting the parameters to simulation data while incorporating design attribute dependencies is considered. The numerical model order reduction approach to macromodeling is presented second, and some of the issues associated with fast solvers and model reduction are summarized. Lastly, we describe the recently developed circuit-based approach for simulating micromachined devices, and describe the design hierarchy and the use of a catalog of parts.

1 Introduction

Decades of enormous research and capital investment in VLSI technology has made it possible to put more than a million transistors on a square centimeter of silicon, and that investment is now also making it possible to fabricate devices with micron-scale moving parts. The specific techniques used to fabricate such vanishingly small moving parts is often referred to as micromachining, and the potential impact of micromachining is hard to understate. Micromachined devices will play a key role in making the now pervasive computer technology interact more directly with the physical world. Micromachined devices are already providing such physical-computer interfaces: micromachined accelerometers are used in automobile automatic airbag deployment systems [1], micromachined million mirror arrays are used in computer projection displays [2], and centimeter-sized pressure sensors are used in a range of industrial control applications [3].

Researchers in almost every engineering and scientific discipline are examining ways to harness the ability to fabricate, at low cost, centimeter-sized systems with of hundreds of thousands of mechanical parts and transistors. Microresonators, which can replace bulky passive components in communication circuits, may usher in wristwatch-sized cell phones (for better or worse) [4]; active research on microfluidic valves, pumps and mixers may lead to single-chip chemical analysis systems which could be used to make "in-vitro" medical diagnostic equipment or pocket-sized chemical agent detectors [5]; research on microfabricated turbines and generators [6] may lead to an alternative to batteries for portable energy; and microfabricated parts small enough to capture and hold individual biological cells will accelerate progress in both medical and scientific research [7].

Over the last decade there has been extensive, and successful, research focussed on developing and exploiting micromachining, though there are very few high-volume micromachined products. In addition, almost all the research in applying micromachining technology has been carried out by specialists with many years of focussed training. In contrast, integrated circuit designers do not need such a high level of specialization. Instead, they rely on a coordinated suite of synthesis and verification tools that makes it possible to design an application-specific circuit with high confidence of first-pass success, even without becoming an expert in semiconductor fabrication. The current situation for micromachined device designers is very different. These designers must know the fabrication process intimately, and may even have to design their own process. In addition, the

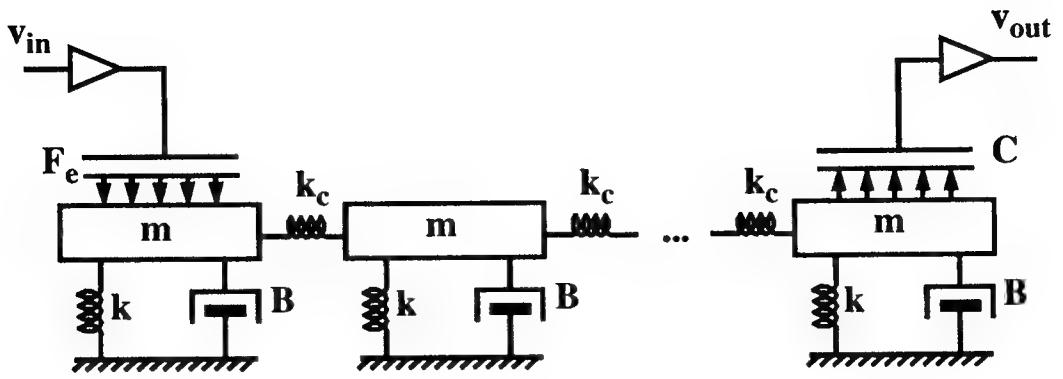

Figure 1: System-level behavioral model of a multi-resonator filter

design tools available are often limited and provide only domain-specific simulation or rudimentary layout editing. The combination of inadequate computer-aided design tools and rapidly evolving process technology has created an expertise barrier that excludes nonspecialists who would bring important application expertise. Unless this expertise barrier is lowered, primarily through vastly improved computer-aided design tools, it seems unlikely that the potential of micromachining to impact so many different disciplines will be achieved.

Although the need for design tools for micromachining has been recognized for well over a decade, progress has been stymied by a problem whose difficulty has been persistently underestimated. To introduce this problem, consider that for nearly thirty years, integrated circuit designers have relied on circuit simulation. This one tool has nearly eliminated the need to build prototype circuits in order to find major design flaws. One reason for the success of circuit simulation is that its input is the same schematic diagram that designers use to reason about the circuit, and the simulator's output is roughly the same as would be produced by prototyping the circuit and then measuring all the voltages and currents. The problem for micromachined designers is that there is no equivalent of a circuit simulator, and no equivalent of a schematic language to describe the device to a simulator, if such a simulator existed. Simulator extension languages like VHDL-AMS [8] can greatly simplify the mechanics of incorporating models for micromachined devices into circuit simulators, but they do not address a more fundamental problem. In a traditional circuit schematic, elements interact only at nodes, and the physical position of elements has limited impact on performance. Neither of these these circuit-oriented concepts translate directly to micromachined device design.

The problem of how best to extend circuit simulation to include micromachined devices is fundamental, and as yet, unsolved. For this reason, in this paper we will focus on the emerging approaches to simulation. In order to make some of the issues clearer, we will start in the next section with a brief description of a filter example which uses a micromachined device. Then in section 3, we will describe the currently most widely used approach to extending circuit simulation, that of generating semi-analytical macromodels for each type of micromachined device. Then, in section 4, we will discuss the desirability and difficulties of replacing the semi-empirical macromodeling approach with a purely numerical approach based on computer simulation and model-order reduction. In section 5, we will approach the simulation problem from the specification side, and discuss a hierarchy of elements and a schematic description for a certain classes of micromachined devices. Finally, in our conclusions, we try to tie together these separate approaches and loosely conjecture about where the field is going.

2 Example and Background

In this section we describe a design example in order to help illustrate the difficulties in developing extensions to a circuit simulator for micromachined devices. The example is a bandpass filter which uses a series of comb-drive micromachined resonators [9], shown in a high-level form in figure 1. The high-level diagram is best described by tracing from input to output. The input v_{in} in figure 1 is connected to a triangle which represents a transistor amplifier. The parallel plates adjacent to F_e indicates an electrical to mechanical conversion. The force F_e accelerates the first mass in a spring-coupled cascade of spring-mass-dashpot resonators. Finally, the parallel plates adjacent to C indicates a mechanical to electrical conversion which feeds an transistor amplifier which generates v_{out}.

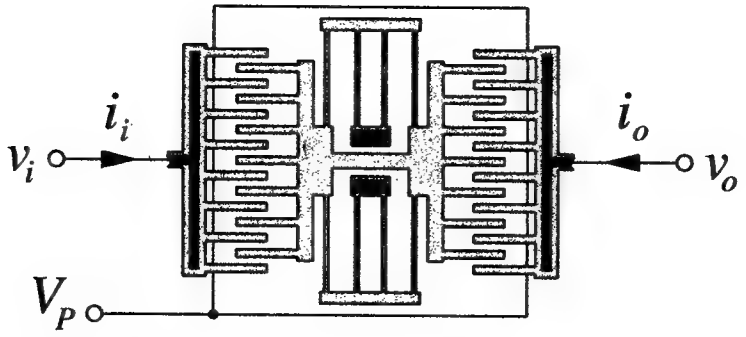

Figure 2: Overhead view of the lateral microresonator (Figure thanks to C. Nguyen and R. Howe, permission not yet confirmed).

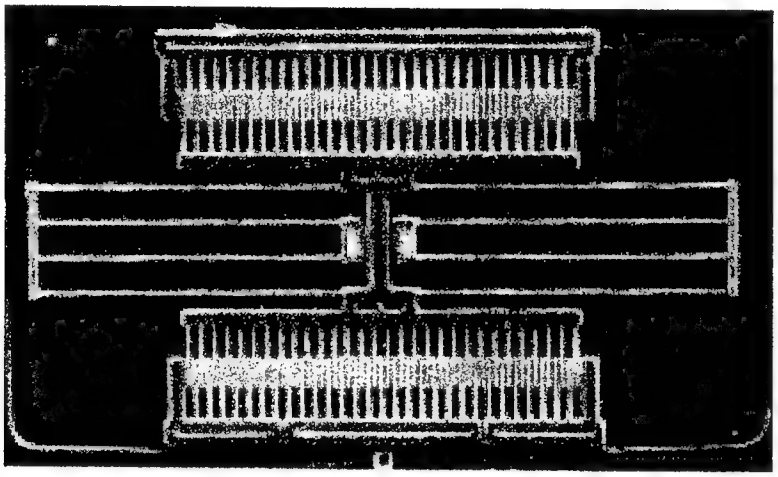

Figure 3: SEM of an integrated CMOS resonator (Figure thanks to C. Nguyen and R. Howe, permission not yet confirmed).

In order to better understand the filter example, consider a single comb-drive lateral microresonator, a layout is shown in figure 2. An SEM of the fabricated device is shown in figure 3. The polysilicon resonator structure, which appears white in the SEM picture and gray in the top view diagram, has been released from the substrate underneath except at certain attachment points. The thick black lines in figure 2 are used to show where the polysilicon structures are attached to the substrate, or anchored. As is clear from figure 2, the structure has three separately anchored parts: a left comb, a right comb, and a dual-comb central shuttle which is anchored to a only through thin polysilicon beams. The thin beams serve two purposes. They act as springs and allow the central shuttle to oscillate from left to right, and they provide a conductive path between the central shuttle and a fixed conducting plate held at a bias potential V_p. The interdigited combs generate electrostatic forces which pull the shuttle to the left when $v_i > v_0$ and to the right when $v_0 > v_i$, assuming both v_i and v_0 are larger than V_p. If out-of-phase sinusoidally varying voltages are applied to v_i and v_0, along with a dc offset, then the amplitude of the central shuttle's steady-state oscillation will be strongly frequency dependent.

As the diagram in figure 2 suggests, all that is needed to include the resonator in a circuit simulator is to determine a relationship between the currents i_i and i_0 and the voltages V_p, v_i, and v_0. And at least formally, the needed current-voltage relationship can be derived by determining the mechanical material properties and then solving a coupled system of time-dependent partial differential equations on a moving boundary. In particular, the shuttle accelerates and the tethers bend elastically in response to forces generated by exterior electric fields and viscous drag. The drag will not be exactly zero if the resonator is packaged in a vacuum, because there are still mechanical energy loss mechanisms which create an effective drag force.

Though the statement in the preceding paragraph is true, it is hides many of the important difficulties. Determining a device's three-dimensional structure and associated material properties requires a detailed

understanding of the fabrication processes as well as a set of carefully designed experiments [10]. Solving coupled systems of three-dimensional time-dependent partial differential equations with a complicated moving boundary requires sophisticated numerical techniques and a great deal of computer time [11, 12]. Finally, developing a current-voltage relation for the resonator in figure 2 may not even be an appropriate goal. To see why, reconsider the original filter with the three stage resonator shown in figure 1. In the multi-stage resonator, the single stage resonators are coupled together by springs which are implemented using thin polysilicon tethers. For the multi-stage resonator, the most important aspect to model well is the transfer function from the input of the first resonator to the output of the last resonator. However, there will be no way to arrive at that transfer function by "composing" the previously mentioned single resonator models. Instead, an entirely new model will be needed for a two-stage resonator, and then another model for a three-stage resonator, and yet another model for a four stage resonator, et cetera. And if these models are going to be derived by solving time-dependent partial differential equations for structures as geometrically complicated as a multistage resonator, the computer time required may cast a more positive light on building prototypes.

In order to assess the importance of issues like deriving structure and material properties from layout and process information, the computational cost of partial differential equation solution, or model composibility, it is worth recalling that for integrated circuit design, simulator use can be divided into two broad classes. Early in the circuit design process, during a ***synthesis or optimization phase***, many alternatives are being considered, and designs are typically represented only with a schematic. That is, circuit element interconnection is specified, but no layout information exists. The simplicity of the schematic representation both builds intuition and accelerates examining alternatives, though layout parasitics are either ignored or crudely estimated. As the design matures, when the circuit layout has been determined, a ***verification phase*** begins. Circuit simulators are then combined with layout extraction techniques to check that the final layout results in a circuit with the desired performance. Such a two stage approach also seems to be a natural fit to designing the microresonator filter. It would be very efficient if most of the layout details could be avoided while examining alternatives such as: fewer or more resonator stages; fewer or more comb fingers; heavier or lighter shuttles; and longer or shorter or more serpentine tethers. Then only during the verification phase would it be necessary to work with the layout and combine extraction techniques with simulation.

3 Semi-Analytical Macromodeling

By far the most common approach to including a micromachined device in circuit simulation is to analyze the device approximately, so as to generate a macromodel in the form of either a circuit or a low-order system of differential equations [13]. Generating the form of these models requires the device designer's physical insight, and can be as much art as science, though issues such as energy conservation can provide guidelines [14]. Once the form of the macromodel has been discerned, then values for the parameters must be determined. These parameters can be determined analytically, or by experiment, or by using numerical simulation. The decomposition between macromodel form and parameterization is not a precise one, and is best described by example. Below, a simple macromodel form for the single resonator example of figure 2 is derived, and then several alternatives for determining model parameters are examined. The merits and deficits of semi-analytic macromodels are then described in general.

3.1 Example Model Form

In order to develop a model for the resonator which can be incorporated in a circuit simulator, the resonator voltages must be related to the resonator currents. Resonators are usually modeled as RLC circuits [9] as such models help develop intuition. A differential equation model is developed below because the setting is more generally applicable. To begin, from figure 2, the currents i_i and i_o can be related to the voltages v_i, v_o and V_p by first noting that

$$i_i(t) = \frac{d}{dt} Q_L(v_i - V_p, x) \quad i_o(t) = \frac{d}{dt} Q_R(v_o - V_p, x) \tag{1}$$

where x is the displacement from center of the dual-comb shuttle, and Q_R and Q_L are the net charges on the left and right anchored combs, respectively. A simple parallel plate analysis suggests that the comb capacitance is an affine function of the displacement x, in which case the comb charges will satisfy an equation of the form

$$Q_L(v_i - V_p, x) \approx (C_0 - C_1 x)(v_i - V_p) \quad Q_R(v_i - V_p, x) \approx (C_0 + C_1 x)(v_o - V_p) \tag{2}$$

where C_0 is the comb-pair capacitance at $x = 0$ and C_1 is the x-derivative of that capacitance. Note that there is only one C_0 and one C_1 so we have exploited the left-right symmetry in the problem. Finally, a very simple

spring-mass mechanical model for the comb suggests that the shuttle displacement, x, satisfies an equation of the form

$$M\frac{d^2}{dt^2}x + K_d\frac{d}{dt}x + K_s x = K_e\left((v_o - V_p)^2 - (v_i - V_p)^2\right) \tag{3}$$

where M is the mass of the shuttle, K_d is the drag force on the comb generated by the surrounding fluid (typically air at room pressure), K_s is the spring constant associated with the thin teathers, and K_e is constant which relates the electrostatic force generated by the comb to the square of the applied voltage.

3.2 Determining Model Parameters

A very simple analysis of the microresonator was used above to develop a differential equation system macromodel. The model is given by the combination of (1), (2), and (3). It is worth noting that the model is nonlinear and has quite a few parameters. Until the parameters are set, there is only a "form" for the macromodel. In the above example, and for macromodels in general, specifying the macromodel form usually implies: assigning a set of state variables, determining which time derivatives appear, representing which state variables interact, and specifying where the parameters appear. It is also quite common to include certain expected nonlinearities, as was done with the squared potential in (3).

The above macromodel has many parameters, C_0, C_1, M, K_d, K_s and K_e, so it is tempting to suggest that the model could fit anything. Since the macromodel is intended only as an example, we will consider the issue of how to determine the parameters rather than focusing on how to improve the model. There are two main issues associated with macromodel parameter selection:

1. *Will the parameters be determined by physical analysis or through fitting to measured or simulated data?*
2. *Will a new set of parameters be determined every time a change is made in the device geometry, or will the parameters be given as an explicit function of design attributes?*

Most macromodels use some combination of analysis and data fitting to determine the parameters. For example, the shuttle mass of the resonator, M, is easily determined from the geometry and material properties, but would be difficult to measure directly. There are techniques for estimating shuttle drag [15], K_d, though recent studies suggest that numerically solving the Stoke's equation yields higher accuracy [16]. Finite-element analysis or measurements might also be superior to trying to use linear beam theory when attempting to determine the spring coefficient K_s [10, 17]. In general, as software for solving partial differential equations improves, parameter estimation will be more heavily based on results from simulation rather analytical techniques.

There are many aspects of a microresonator that a designer can alter to try to improve performance including: the number and length of comb fingers, the tether lengths and widths, and the shuttle proof mass. One advantage of using physical analysis to determine macromodel parameters is that the analysis usually reveals an explicit form for the dependence of the parameters on design attributes. Macromodels whose parameters are given as explicit functions of design attributes are of obvious value during the synthesis and optimization phase of design. If the electrostatic force constant, K_e, is estimated analytically using a parallel-plate formula, then the resulting formula for the parameter K_e will include a term which grows linearly with the number of comb fingers.

Deriving macromodel parameters by fitting to measured data or simulation results does not preclude generating macromodels whose parameters are given as explicit functions of the design attributes. It is possible to use a multivariate polynomial fitting procedure to generate these explicit functions, but the procedure is not completely automatic and requires expert input [17]. To understand the difficulty, consider a micromachined device whose macromodel has a parameter P that is dependent on the value of d design attributes. We will denote the values of the d design attributes as a d-length vector u. Then, our problem becomes one of determining an explicit representation of $P(u)$.

A seemingly straight-forward approach to finding an explicit representation of $P(u)$ is to use a multivariate polynomial. To see the difficulty generated by such an approach, consider all the terms of a second-order polynomial in three design attributes,

$$\begin{aligned} P(u) = \quad & \beta_0 + \beta_1 u_1 + \beta_2 u_2 + \beta_3 u_3 + \beta_4 u_1 u_1 + \beta_5 u_1 u_2 \\ & + \beta_6 u_1 u_3 + \beta_7 u_2 u_2 + \beta_8 u_2 u_3 + \beta_9 u_3 u_3, \end{aligned} \tag{4}$$

where $u = [u_1 u_2 u_3]^T$ are the design attributes and the β_i's are the unknown coefficients of the multivariate polynomial. As should be clear from the above example, the number of terms in a q^{th} order d-dimensional

polynomial is proportional to d^q. This implies that it will be computationally hopeless to use multivariate polynomials directly to represent parameter variation when the number of design attributes exceeds a half dozen. Instead, the polynomials will have to be modified by "pruning" unnecessary terms. Determining which terms can be safely discarded requires significant mathematical and physical insight.

There is a second issue associated with fitting $P(u)$ with a polynomial, and this issue is sometimes referred to as the "design-of-experiments" problem. Consider again the problem of fitting $P(u)$ with a second-order polynomial in three design attributes. In order to compute the ten unknown polynomial coefficients $\beta_0, ..., \beta_9$, values for $P(u)$ must be computed for at least 10 different values of the 3-length vector u. There are several approaches to determining the "best" test values for u [17] based on statistical arguments, but the key difficulty and its cure can be seen by examining the matrix equation associated with the fitting. Again for our second-order example, assume there are $l+1$ measurements, $l \geq 9$, and let the measurements (either real or from simulation) be at points u^i for $i = 0$ to l. The matrix equation for the β's is then given by

$$\begin{bmatrix} P(u^0) \\ P(u^1) \\ \vdots \\ P(u^l) \end{bmatrix} = \begin{bmatrix} 1 & u_1^0 & u_2^0 & \dots & u_3^0 u_3^0 \\ 1 & u_1^1 & u_2^1 & \dots & u_3^1 u_3^1 \\ & \vdots & & & \vdots \\ 1 & u_1^l & u_2^l & \dots & u_3^l u_3^l \end{bmatrix} \begin{bmatrix} \beta_0 \\ \beta_1 \\ \vdots \\ \beta_9. \end{bmatrix} \tag{5}$$

Note that the system will be square when the number of measurements equals the number coefficients, though typically the number of measurements far exceeds the number of coefficients.

As is clear from examining (5), the points u_0 through u_l should be chosen to make the rows (or the columns) of the matrix in (5) as close to mutually orthogonal as possible. Finding values of u^i's which generate a nearly orthogonal matrix can be accomplished using a one test point at a time algorithm.

3.3 Merits and deficits

The semi-analytic approach to macromodeling is in far wider use than the methods to be described below. And, since this method is "free-form", there are no restrictions as to what kind of micromachined devices can be modeled. In addition, if such macromodels are carefully parameterized, they can be used to excellent effect during the synthesis and optimization phase of design.

There are two difficulties with the semi-analytic macromodeling approach. The most obvious problem is that there is no standard method for generating these macromodels, and the only way to determine when the models are sufficiently accurate is by comparing the macromodel's results to those of experiments or very detailed simulation. The second problem is simply that the macromodeling approach provides very little verification. One can not "extract" the macromodel from layout, or add in parasitics. In addition, since the device designer usually generates the macromodel, there is no independent check on whether an important interaction is being ignored.

4 Numerical Macromodeling

When the first- and second-order behaviors of a micromachined device are well-understood, the most efficient strategy for including the device in a circuit simulator is to develop the kind of semi-analytic macromodel discussed in the previous section. Given how rapidly the micromachining technology is changing, it is rarely possible to wait for such device expertise to develop. And since it is almost impossible to design systems which use micromachined devices without access to reliably accurate macromodels, slow macromodel development translates into slow technology deployment. For this reason, there has been a steady effort over the last decade to develop nearly automatic approaches for generating accurate macromodels of micromachined devices starting from only layout and process descriptions. Most efforts is this area are following a three step approach: [18, 11, 19]

- Use modified extrusion to generate an approximate 3-D structure from a layout and process description [10, 20].
- Use fast coupled-domain 3-D simulation techniques to analyze the entire micromachined device [12, 21].
- Use a projection-based model-order reduction strategy to generate macromodels from 3-D simulation [22].

Below we describe some of the recent developments and persistent challenges in fast coupled-domain simulation and model-order reduction.

4.1 Fast Coupled-domain 3-D Solvers

The above strategy for generating macromodels by performing projection-based model-order reduction relies on the ability to simulate an entire micromachined device in a reasonable period of time. In order to simulate the microresonator in figure 2, for example, it is necessary to solve a complicated three-dimensional moving boundary problem which couples elastic, fluidic and electrostatic forces. Simulating such problems with standard finite-element methods is nearly intractable, because it is necessary to discretize the volume in both the interior and exterior of the resonator. In order to simulate entire micromachined devices, it was first necessary to develop faster techniques for analyzing the exterior field problems. Then, it became necessary to develop robust approaches for coupling those fast techiques to standard finite-element algorithms for computing elastic deformation.

4.1.1 Fast Field Solvers

For most micromachined devices, the electrostatic and fluidic forces in the exterior of the device satisfy linear partial differential equations. Specifically, the surface electrostatic forces can be determined by solving an exterior Laplace's equation and the fluid drag forces can be determined by solving an exterior Stoke's equation. For both equations, it is possible to derive integral formulations which avoid the exterior volume entirely and instead relates potentials to forces in the electrostatic case, and velocities to forces in the fluid case.

More specifically, the electrostatic potential and the fluid velocity, assuming Stoke's flow, both satisfy an integral equation over the device surface given by Green's theorem:

$$u(x) = \int_{surfaces} G(x,x') \frac{\partial u(x')}{\partial n} \; + \; \frac{\partial G(x,x')}{\partial n} u(x') da', \tag{6}$$

where u is either the electrostatic potential or the fluid velocity, x is a point on the surface, and $\frac{\partial}{\partial n}$ is the derivative in the direction normal to the polysilicon surface.

Discretization of the above integral equation leads to a dense system of equations which becomes prohibitively expensive to form and solve for complicated problems. To see this, consider the electrostatics problem of determining the surface charge given the potential on conductors. A simple discretization for the electrostatics problem is to divide the polysilicon surfaces into n flat panels over which the charge density is assumed constant. A system of equations for the panel charges is then derived by insisting that the correct potential be generated at a set of n test, or collocation, points. The discretized system is then

$$Pq = \Psi \tag{7}$$

where q is the n-length vector of panel charges, Ψ is the n-length vector of known centroid potentials. Since the Green's function for electrostatics is the reciprocal of the separation distance between x and x',

$$P_{i,j} = \int_{panel_j} \frac{1}{4\pi\epsilon \|x_i - x'\|} da', \tag{8}$$

and therefore every entry in P is nonzero.

If direct factorization is used to solve (7), then the memory required to store the matrix will grow like n^2 and the matrix solve time will increase like n^3. If instead, a preconditioned Krylov-subspace method like GMRES [23] is used to solve (7), then it is possible to reduce the solve time to order n^2 but the memory requirement will not decrease.

In order to develop algorithms that use memory and time that grows more slowly with problem size, it is essential *not* to form the matrix explicitly. Instead, one can exploit the fact that Krylov-subspace methods for solving systems of equations only require matrix-vector products and not an explicit representation of the matrix. For example, note that for P in (7), computing Pq is equivalent to computing n potentials due to n charged panels and this can be accomplished approximately in nearly order n operations [24, 25]. To see how to perform such a reduction in cost, consider Figure (4). The short-range interaction between close-by panels must be computed directly, but the interaction between the cluster of panels and distant panels can be approximated. In particular, as Figure (4) shows, the distant interaction can be computed by summing the clustered panel charges into a single multipole expansion (denoted by M in the figure), and then the multipole expansion can be used to evaluate distant potentials.

Several researchers simultaneously observed the powerful combination of integral equation approaches, Krylov-subspace matrix solution algorithms, and fast matrix-vector products [26, 32]. Perhaps the first

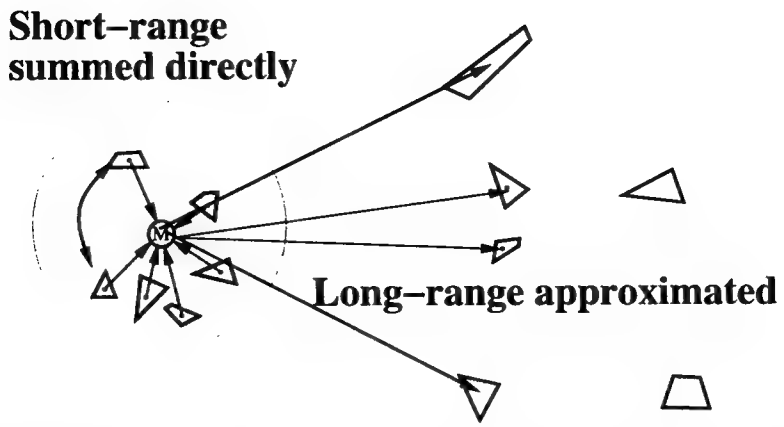

Figure 4: A Cluster of collocation points separated from a cluster of panels

practical use of such methods combined the fast multipole algorithms for charged particle computations with the above simple discretization scheme to compute 3-D capacitance and electrostatic forces [27]. Higher-order elements and improved efficiency for higher accuracy have been the recent developments [21, 31]. The many different physical domains involved in micromachined devices has focussed attention on fast techniques which are Green's function independent, such as the precorrect-FFT schemes [25, 29].

4.1.2 Coupled-Domain Simulation

Self-consistent electromechanical analysis of micromachined polysilicon devices typically involves determining mechanical displacements which balance elastic forces in the polysilicon with electrostatic pressure forces on polysilicon surface. The technique of choice for determining elastic forces in the polysilicon is to use finite-element methods to generate a nonlinear system equations of the form

$$F(u) - P(u,q) = 0. \tag{9}$$

where u is a vector of finite-element node displacements, F relates node displacements to stresses, and P is the force produced by the vector representing the discretized surface charge q. Note that as the structure deforms, the pressure changes direction, so P is also a function of u. One can view this mechanical analysis as a "black box" which takes an input, q, and produces an output u as in

$$u = H_M(q). \tag{10}$$

In order to determine the charge density on the polysilicon surface due to a set of applied voltages, one can use a fast solver, as described above. One can view the electrostatic analysis as a "black box" which takes, as input, geometric displacements, u, and produces, as output, a vector of discretized surface charges, q, as in

$$q = H_E(u). \tag{11}$$

Self-consistent analysis is then to find a u and q which satisfies both (10) and (11).

A simple relaxation approach to determining a self-consistent solution to (10) and (11) is to successively use (10) to update displacements and then using (11) to update charge. Applying (10) implies solving the nonlinear equation, (9), typically using Newton's method.

Although the relaxation method is simple it often does not converge. Instead one can apply Newton's method to the system of equations

$$\begin{bmatrix} q \\ u \end{bmatrix} - \begin{bmatrix} H_E(u) \\ H_M(q) \end{bmatrix} = \begin{bmatrix} 0 \\ 0 \end{bmatrix} \tag{12}$$

in which case the updates to charge and displacement are given by solving

$$\begin{bmatrix} I & -\frac{\partial H_E}{\partial u} \\ -\frac{\partial H_M}{\partial q} & I \end{bmatrix} \begin{bmatrix} \Delta q \\ \Delta u \end{bmatrix} = - \begin{bmatrix} q - H_E \\ u - H_M \end{bmatrix} \tag{13}$$

The above method is referred to as a multi-level Newton method because forming the right-hand side in (13) involves using Newton's method to apply H_M.

In order to solve (13), one can apply a Krylov-subspace iterative method such as GMRES. The important aspect of GMRES is that an explicit representation of the matrix is ***not*** required, only the ability to perform matrix-vector products. As is clear from examining (13), to compute these products one need only compute $\frac{\partial H_M}{\partial q}\Delta q$ and $\frac{\partial H_E}{\partial u}\Delta u$. These products can be approximated by finite differences as in

$$\frac{\partial H_M}{\partial q}\Delta q \approx \frac{H_M(q+\alpha\Delta q) - H_M(q)}{\alpha} \tag{14}$$

where α is a very small number. Therefore, this matrix-free multilevel-Newton method [34] can treat the individual solvers as black boxes. The black box solvers are called once in the outer Newton loop to compute the right hand side in (13) and then called once per each GMRES iteration. Computing $H_M(q+\alpha d_1)$ means using an inner loop Newton method to solve (9), which is expensive, though improvements can be made [12]. An important advantage of matrix-free multilevel-Newton methods is that it is not necessary to modify either the mechanical or electrostatic analysis programs.

4.1.3 Analyzing a Micromachined Resonator

In order to demonstrate that the above techniques make it computationally feasible to simulate an entire resonator, we now present results from a multilevel-Newton coupled electromechanical solver [30]. The program uses the precorrected-FFT accelerated integral equation solver [29] with planar triangular panels to compute the electrostatic forces. A finite-element, mixed rigid/elastic mechanical analysis program using 20 noded isoparametric brick elements [33] is used to compute displacments. The multilevel-Newton method uses to pressure sensitivites to improve efficiencies.

An eighteen finger polysilicon resonator is shown in Figure 5. In this resonator, the central shuttle is is suspended by 400 micron long folded beams with a uniform thickness of 1.94 microns and finger dimensions of 13.8x4.6 microns. The central shuttle and an underside fixed plate (not shown) were set to zero volts, and a drive voltage was applied to the right- and left-hand side combs (also not shown). For this example, the Young's modulus of the polysilicon was determined to be $150MPa$, and the poisson ratio was 0.3.

The effect of varying the separation of the suspension beams, shown as L in Figure 5, on levitation was investigated using the coupled-domain solver. The results are plotted in Figure 6, which shows levitation (motion normal to the substrate) as a function of applied comb drive voltage. Levitation in resonators is to be avoided, because raising the central shuttle causes a misalignment of the interdigitated fingers. This misalignment reduces the resulting electrostatic forces, and may also allow the central shuttle to twist and collided with the side combs. The simulation results plotted in Figure 6 show that levitation in the resonator is can be nearly as large as the resonator thickness, and that changing separation L of the suspension beam inperceptibly effects levitation. The simulation was run on a Sun Ultra 30, and each load step required 70 minutes of CPU time.

4.2 Model-Order Reduction

Many micromachined devices are nonlinear, and extracting dynamically accurate nonlinear macromodels from simulation is a relatively open problem. For this reason, there has been much current interest in developing nonlinear model-order reduction strategies [35, 36, 37]. To better describe the challenges in nonlinear model-reduction, consider simulating the dynamics of a fixed-fixed beam in a fluid (air). Figure 7 [38] shows the front view of the structure. When a voltage is applied, the flexible top plate deforms downward due to the generated electrostatic force, and the squeezed air in the gap damps the plate motion through a back pressure force. The exact deformation of the top plate due to the applied voltage is sensitive to the ambient pressure of the air, so this structure can be used as a pressure sensor.

Following Hung *et al* [38], the dynamic behavior of this coupled electro-mechanical-fluid system can be modeled with the $1D$ Euler beam equation (15) and the $2D$ Reynold's squeeze film damping equation (16):

$$EI\frac{\partial^4 u}{\partial x^4} - S\frac{\partial^2 u}{\partial x^2} = F_{elec} + \int_0^w (p - p_a)dz - \rho\frac{\partial^2 u}{\partial t^2} \tag{15}$$

$$\nabla\cdot(u^3 p\nabla p) = \frac{12\mu}{1+6K}\frac{\partial(pu)}{\partial t}. \tag{16}$$

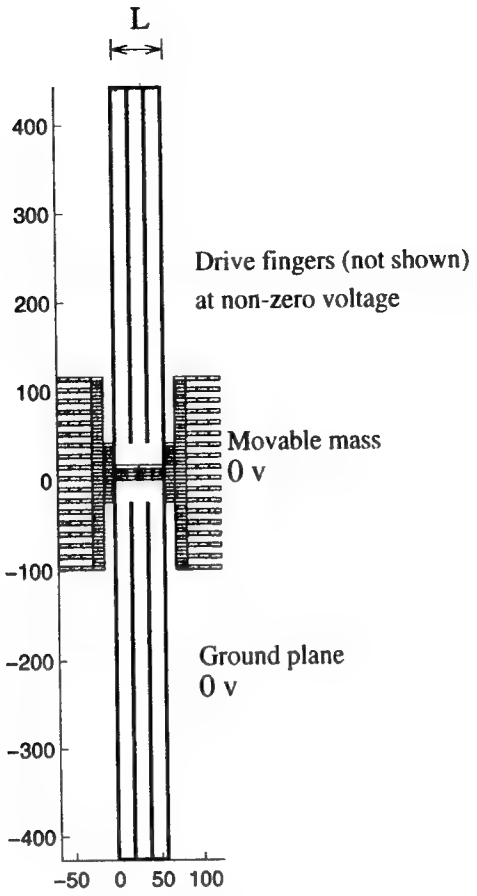

Figure 5: Comb drive resonator

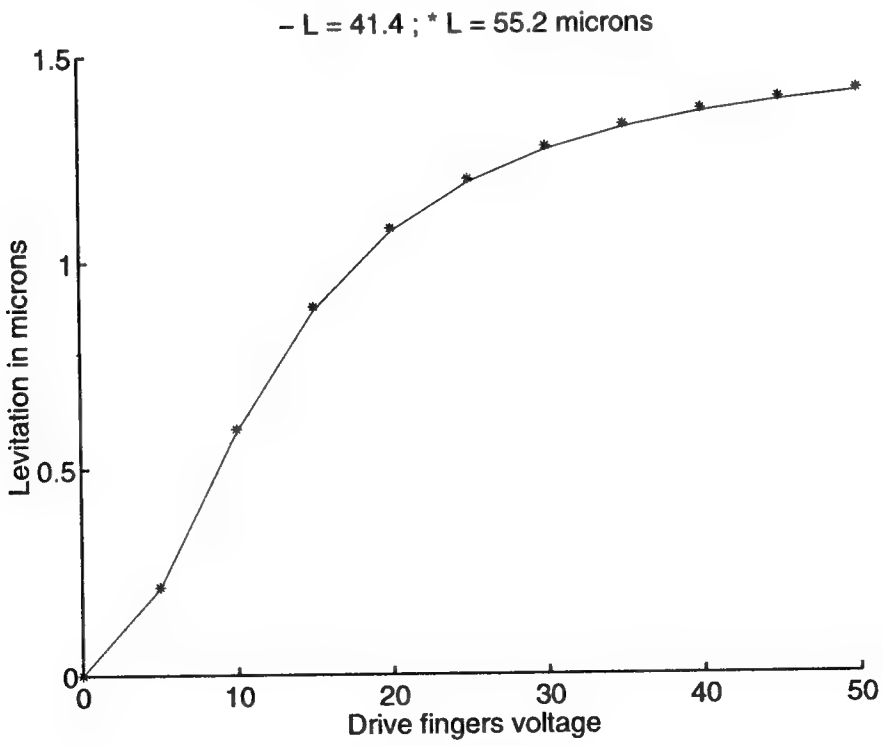

Figure 6: Levitation

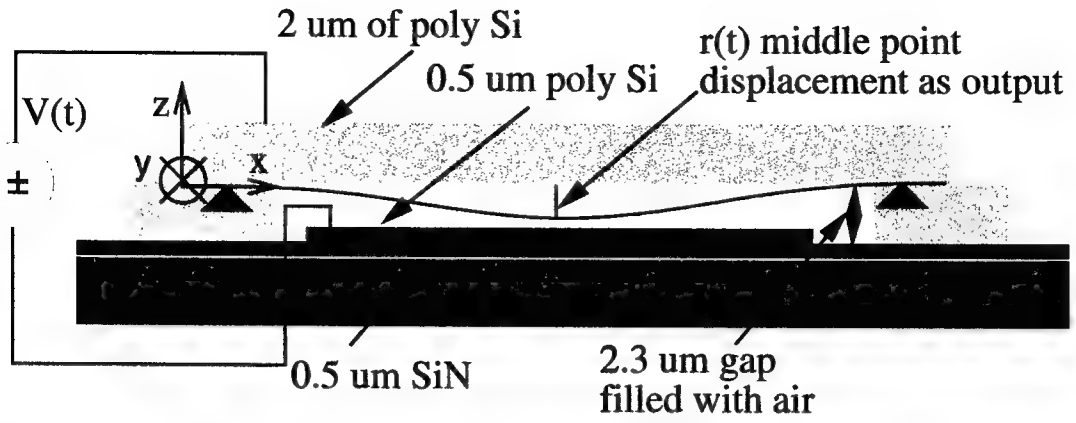

Figure 7: The fixed-fixed beam structure. The x and z axes are parallel to the length and width of the beam, respectively, and the y axis points into the page.

where x, y and z are as shown in Figure 7, E is the Young's modulus, I is the moment of inertia, S is the stress coefficient, ρ is the density, p_a is the ambient pressure, μ is the viscosity, K is the Knudsen number, w is the width of the beam in the y direction, $u = u(x,t)$ is the height of the beam above the substrate, and $p(x,y,t)$ is the pressure distribution in the fluid. Finally, the electrostatic force is approximated assuming nearly parallel plates and is given by $F_{elec} \cong -\frac{\epsilon_0 w V^2}{2u^2}$ where V is the applied voltage.

Spatial discretization of (15) and (16) leads to a large nonlinear system of the form

$$\dot{\mathbf{x}} = \mathbf{f}(\mathbf{x}) + \mathbf{b}^{\mathbf{T}}\mathbf{u}(\mathbf{t}) \quad y = \mathbf{c}^{\mathbf{T}}\mathbf{x} \tag{17}$$

were $\mathbf{x}$ is an n-length state vector, in this case the vector of displacements and their time-derivatives. The function $\mathbf{f}$, which maps an n-length vector to an n-length vector, represents the spatially discretized partial differential equation. The above system with a nonlinear state equation is referred to as the "original" system which will be reduced to a much smaller system. The applied voltage generates $u(t)$, the input of the system. The output of the system is $y(t)$, and is chosen to be the beam's center point displacement.

4.2.1 Numerical Model Reduction

The goal of numerical model-order reduction is to generate a model with many fewer than n states which still preserves the input/output behavior of the original system. Almost all the numerical model-order reduction strategies are based on a change of variables,

$$V_q x_q = x, \tag{18}$$

where x_q is a q-length vector (q is assumed much much less than n), and V_q is $n \times q$ orthonormal matrix whose columns represent important "modes". Then, the matrix V_q represents a transformation from the original to the reduced coordinate system. Substituting the change of variables in (17) and multiplying the resulting equation by V_q^T yields

$$\dot{x_q} = V_q^T f(V_q x_q) + V_q^T b u(t) \quad y = c^T V_q x_q. \tag{19}$$

It should be noted that the dynamical system could have been multiplied by a second transformation matrix, U_q, leading to a wider range of algorithms.

Buried in (19) are the two key model-order reduction issues. First, one must select a good change of variables so that the input/output behavior is captured by the q states in the reduced system. Second, and perhaps less obvious, one must have a representation of $V_q^T f(V_q \cdot)$ that can be efficiently stored and evaluated. For example, suppose $n = 100,000$ and $q = 10$. Then computing $V_q^T f(V_q x_q)$ explicitly would require on the order of $100,000$ operations, and that hardly satisfies the efficiency goal of model-order reduction. If f were linear, so that $f(x) = Ax$ where A is an $n \times n$ matrix, then the representation problem is easily solved. To see this, consider that for the linear case

$$f_q(x_q) \equiv V_q^T f(V_q x_q) = V_q^T A V_q x_q = A_q x_q, \tag{20}$$

where $f_q(\cdot)$ is a function which maps a q-length vector to a q-length vector and denotes the general nonlinear representation of the reduced model in the reduced variables. The matrix A_q is a representation of the reduced

model which can be used when the problem is linear. As is clear from the equations, A_q is an easily computed $q \times q$ matrix. For the example numbers above, using the A_q matrix representation to compute $V_q^T f(V_q x_q)$ costs only 100 operations instead of order 100,000.

Returning to the first issue, selecting the change of variables or equivalently chosing V_q, there are a number of methods. If the problem is linear, the methods for determining V_q include: examining Krylov-subspaces [39, 22, 40], selecting from orthogonalized time-series data [35], or computing singular vectors of the underlying differential equation Hankel operator [41]. The approach based on using time-series data extends directly to the nonlinear cases, and the Krylov-subspace and Hankel operator approaches can be extended to the nonlinear case by linearizing the system only for the purpose of computing V_q, and then applying the change of variables to the original nonlinear system. As shown in [37], linearization approaches can be ineffective and better strategies may exist.

Regardless of how the V_q's are computed, for nonlinear problems there is still the difficulty of finding an efficient representation for $V_q^T f(V_q \cdot)$. One approach is to assume the reduced model is a multidimensional quadratic [43, 42], in which case

$$V_q^T f(V_q x_q) = f_q(x_q) \approx J_q^{(1)} x_q + x_q^T J_q^{(2)} x_q \tag{21}$$

where $J_q^{(1)}$ is the $q \times q$ Jacobian, or first derivative, of f_q and $J_q^{(2)}$ is a $q \times q \times q$ second derivative of f_q. Both $J_q^{(1)}$ and $J_q^{(2)}$ are easily computed from f by finite-differences, though q^2 function evaluations are needed to evaluate $J_q^{(2)}$ [42]. If higher order nonlinearities are required, such as cubic or quartic terms, the above strategy becomes computationally ineffective. The difficulty arises from the fact that there are q^{k+1} entries in the k^{th} derivative of f_q, so generating a tenth-order reduced-order model and including all the quartic terms requires a representation with over 100,000 entries. It is possible to use heuristics to prune the higher-order nonlinearities, so that only a small fraction of the q^{k+1} terms are retained. Equivalently, the problem is one of determining a sparse representation for $J_q^{(k)}$.

An alternative view of the nonlinear model reduction problem can be developed for the case where the original nonlinear function, f, can be represented as the gradient of a scalar function [45]. That is,

$$f(x) = \nabla_x \phi(x) \tag{22}$$

where ϕ maps an n-length vector to a scalar. Such representations occur naturely for second-order energy-conserving systems,

$$\ddot{x} = \nabla_x \phi(x) + b^T u(t), \tag{23}$$

where $\phi(x)$ is derived by constructing the system's associated Hamiltonian. For such systems, the representation problem can be reduced to a single fitting problem by noting that

$$f_q(x_q) = V_q^T f(V_q x_q) = V_q^T \nabla_x \phi(V_q x_q) = \nabla_{x_q} \phi_q(x_q), \tag{24}$$

where ϕ_q maps an q-length vector to a scalar. Then, the scalar function of q variables, ϕ_q, can be approximately represented using a q-dimensional k^{th}-order polynomial

$$\phi_q(x_q) \approx \sum_{i_1=0}^{R_1} \cdots \sum_{i_k=0}^{R_k} a_{i_1,\ldots i_k} {x_{q_1}}^{i_1} \ldots {x_{q_q}}^{i_k}. \tag{25}$$

If one represents f directly using derivatives, as in the previous paragraph, there are order q^{k+1} terms in the reduced model. Using a polynomial to represent ϕ up to order k requires only order q^k terms, so it would seem that exploiting $f = \nabla\phi$ results in a saving of only a factor of q. However, one can fit ϕ with a rational function

$$\phi_q(x_q) \approx \frac{\sum_{i_1=0}^{R_1} \cdots \sum_{i_k=0}^{R_k} a_{i_1,\ldots i_k} {x_{q_1}}^{i_1} \ldots {x_{q_q}}^{i_k}}{\sum_{i_1=0}^{R_1} \cdots \sum_{i_k=0}^{R_k} b_{i_1,\ldots i_k} {x_{q_1}}^{i_1} \ldots {x_{q_q}}^{i_k}}. \tag{26}$$

and rational function representations can be effectively much higher order than k without the commersurate increase in cost [45].

4.2.2 Clamped beam example

We now present the results of comparing the reduced-order models generated using the Arnoldi method and a finite difference solution of the original non-linear governing equations which is provided by Hung [38]. Hung verified this non-linear solution with experimental data.

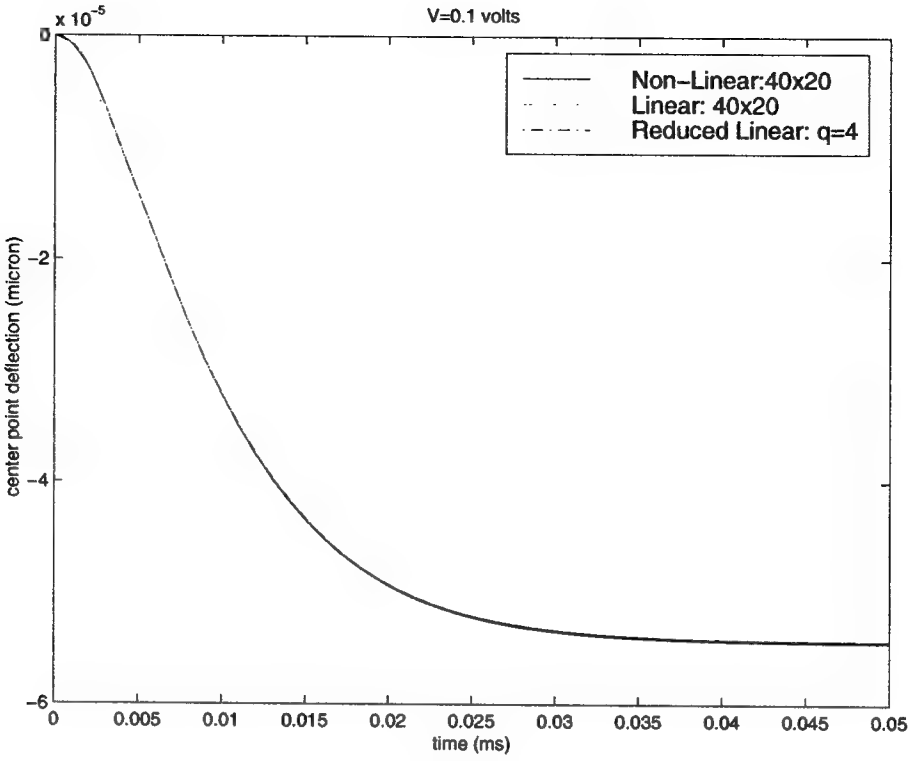

Figure 8: A comparison of the time responses of the non-linear model, linear model and 4th order reduced model at small voltage input $V = 0.1volts$. The center point displacement is plotted against time.

With the mesh size of 40×20, an 880th order system was generated by the linearization process, i.e. 880 ODE's. We compare the time history of the displacement of the center point of the beam at different step input voltages: 0.1V, 2V and 9V. Three models are compared, namely, the full finite difference solution of the original non-linear model of equations, the linearized system of equations, and a 4th order reduced model generated using a Krylov-subspace method for selecting V_q. Figure 8 shows that for a small input voltage $V = 0.1volts$ the three curves representing solutions of each of the three models overlap with one another. The figure shows that with such a small input voltage the original system behaves almost perfectly linearly, and that the 4th order reduced model faithfully reproduces the behavior of the 880th order linear system.

In Figure 9, we see that the linearized model starts to deviate from the non-linear model, but the 4th order reduced model still follows the linear model nearly exactly. Figure 10 demonstrates that at the pull-in voltage, the time response of the structure is extremely non-linear. The linear model and the 4th order macro-model are only accurate during the initial part of the transient.

For a discretization size of 10×5, which is in turn a 70th order linear system, we compared the frequency responses of the linear model and various orders of Arnoldi based macro-models. Figure 11 shows the comparison of the frequency responses of the large linear system and two macro-models that are of the order of 2 and 10, respectively. We see from Figure 11 that the original linear system is a well damped system. The original linear system has a bandwidth frequency of 1.8×10^5.

This figure also shows that the 2nd order macro-model perfectly matches the linear model in a low frequency range up to $10^6\,Hz$. And the 10th order model is able to follow all the oscillatory behavior both in the gain plot and the phase plot. The frequency-domain accuracy of the 10th order model would be important if the device where part of a feedback system.

5 A Circuit Representation for Micromachined devices

The semi-analytical macromodeling approach can be quite effective for design synthesis and optimization, but given the macromodel has built-in assumptions about device behavior, the approach is not a very effective verification strategy. The numerical model-order reduction approach, even if the difficulties with nonlinearities

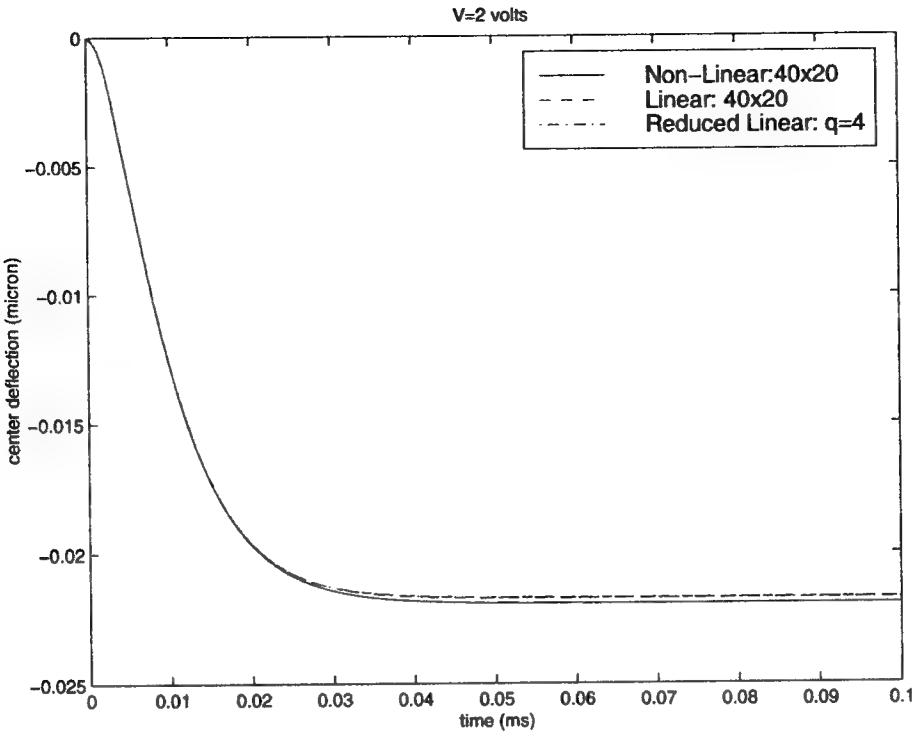

Figure 9: At $V = 2volts$, the linear model starts to deviate from the non-linear model. The reduced-order model still follows the linear model.

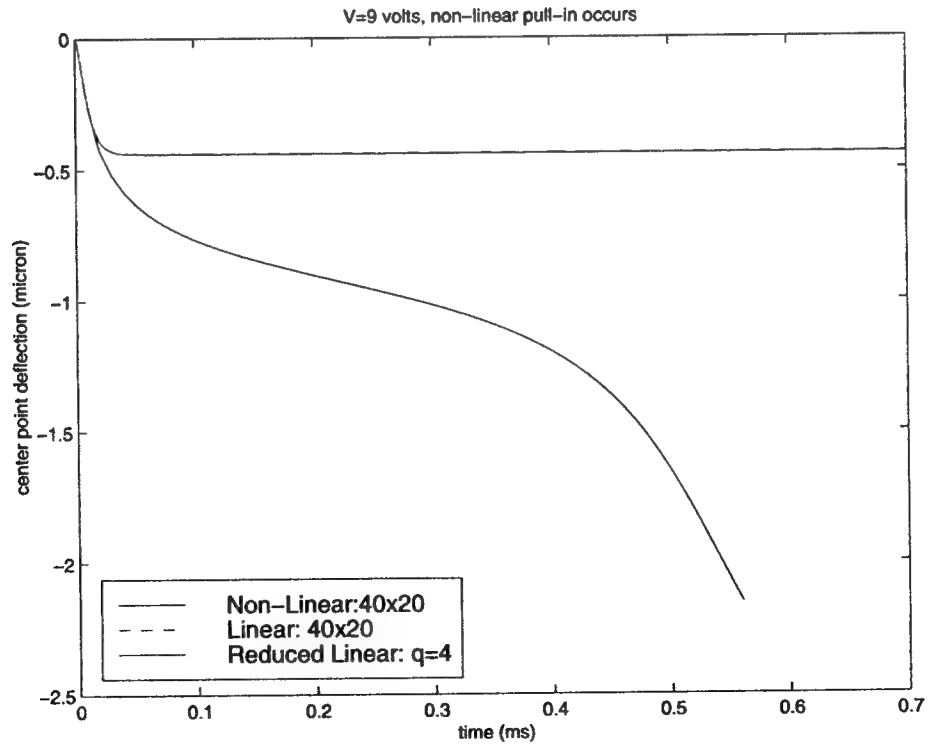

Figure 10: A comparison of the time responses of the non-linear model, linear model and 4th order reduced model at small voltage input $V = 0.1volts$. The center point deflection is plotted against time.

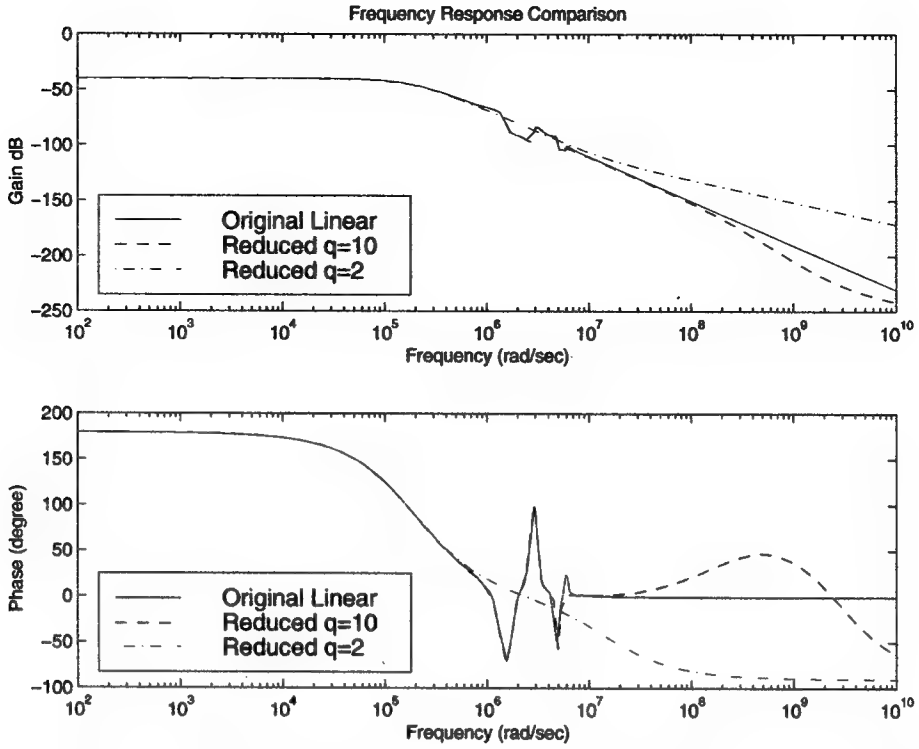

Figure 11: A comparison of the frequency responses of the full linear system, 2nd order reduced model and 10th order reduced model.

were overcome, seems poorly suited to the synthesis and optimization phase of a design because the approach requires a complete layout of the device, and it yields no information about sensitivities to changes in design attributes. In this section we will describe a third alternative to extending circuit simulation to include micromachined devices. An approach will be developed which comes much closer to providing a schematic-like description for micromachined devices, but at the cost of narrowing the range of micromachined devices which can be so treated. So in that sense, this circuit-like description intended to make simulation easier is also a step towards top-down or structured design methodologies [46, 47, 48, 49, 50, 51, 52, 53, 54].

Developing a circuit representation for micromachined devices involves determining the list of elements for the circuit representation, the model for each element, and the definition of the nature or discipline for the terminals of the elements. The goals in selecting the list, model and nature include design reuse and simulation accuracy. Element parameterization provides both, while supporting a wide class of micromachined device designs. Parameterization with both design attributes and process parameters (captured in the model technology file) allows process independent models that can be used to simulate devices in a variety of fabrication lines. A conservative Kirchhoffian network representation is used both for simulation accuracy, and for compatibility with electronics design. Signal-flow representations, commonly used for behavioral or system-level modeling, are more cumbersome to use for this application because they are based on unidirectional elements while mechanical and electrical components interact bidirectionally.

5.1 Element Hierarchy

Micromachining technology combines sacrificial etching with VLSI-style deposit, pattern and etch sequences to produce miniaturized mechanical components that are suspended, cavitied, hinged, or otherwise mounted. The circuit approach described below focuses primarily on suspended microstructural devices as that is the most mature micromachining design space. In principle, the circuit approach can be extended to include hinged structures for optical applications or cavitied structures for fluidic applications.

Suspended micromachined devices involve plates tethered by beams to anchors. Air gaps between conductive micromachined elements act as a variable sensing capacitance and a source for electrostatic actuation force. For example, plates can be actuated electrostatically to tilt micromirrors in digital computer

Figure 12: Atomic elements for design of suspended micromachined systems include (a) anchor, (b) beam, (c) gap and (d) plate.

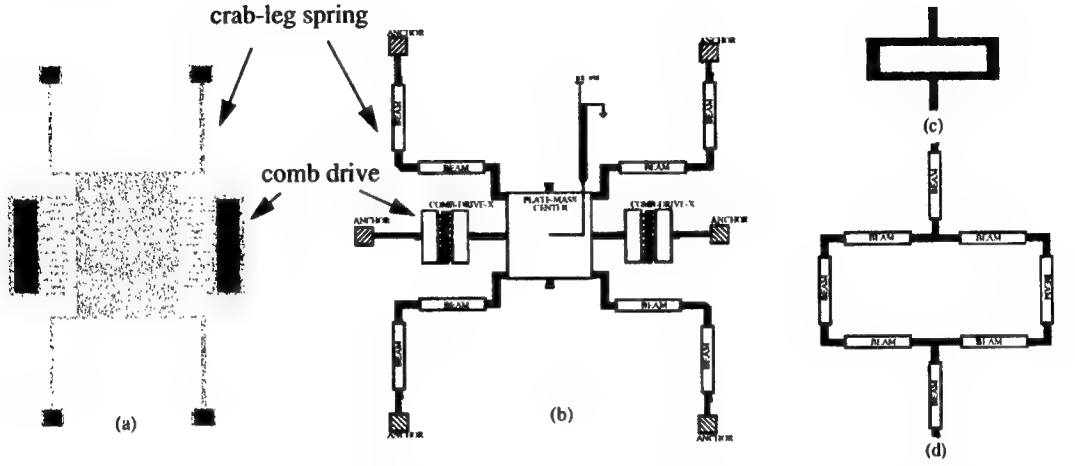

Figure 13: (a) Layout and (b) Schematic Representation of an individual crab-leg microresonator; and (c) Layout and (d) Schematic representation of "O" coupling spring.

projection displays [2] or in optical switches. Micromachined inertial sensors employ one or more plates as proof masses, which move when accelerated and whose motion is sensed capacitively [55]. Such suspended micromachined structures decompose into anchors, beams, plates and gaps, as shown parametrized in Figure 12. This set of elements is chosen for three reasons: they all occur commonly (albeit sized by appropriate geometric parameters); they are modular (in the sense that they are decoupled from neighboring elements); and their behavior can be accurately approximated with a simple lumped parameter model. For the class of Manhattan-geometry suspended polysilicon devices, this set of four elements completely covers the possible design space, and forms a set of atomic basis elements in the circuit representation.

A circuit simulation environment for micromachined devices based on this element library with parametrized behavioral models, called NODAS (Nodal Design of Actuators and Sensors), has been developed [56, 57, 60]. Schematic examples of a crab-leg resonator and an O-shaped spring using the basis elements are shown in Figure 13. The use of circuit element libraries for nodal analysis of micromachined systems [64, 65, 66] and for microgyroscope simulation [58, 67] are also being simultaneously pursued.

Circuit representation of additional elements at higher levels of the hierarchy may also be desirable, primarily because such elements aid in the capture of complex designs. In particular, the parameterized functional elements such as the linear comb-drive sensor or actuator, or the crab-leg spring, O-spring, or folded-flexure spring are easily re-used because they capture a single function (generate electrostatic force, provide mechanical stiffness, etc.) and hence can be accurately represented by behavioral models. While parametrized models at high levels of component abstraction are still possible, the fixed topology of these components limits their re-usability. Moreover, the large number of design variables in such abstractions significantly increases the complexity of generating a parametrized lumped-parameter model as detailed in Section 3.2.

In addition to carefully choosing the elements in the design library to ensure richness of coverage of the design space, the terminals of each element needs to be carefully chosen to balance the need for interoperability between the elements and the accuracy and speed of design simulation. By using the same terminal natures at all levels of the design hierarchy, a composable design representation for mixed-level simulation is possible. This is particularly important as simulation of entire systems at the atomic level, though possible, may require

unnecessary long simulation times. A library consisting of the most common atomic and functional elements therefore supports both rapid simulation as well as the capability to represent a wide class of designs.

As the underlying simulation representation is a Kirchhoffian network, the nature of the quantity defined *across* and *through* each branch in the network is very important. In the electrical domain, voltage across and current through a branch is the accepted standard. For mechanical domains, no standard nature exists. Two possible translational mechanical across-through relations are velocity-force and displacement-force. The latter representation is preferred in micromechanical design, as displacement is generally the most common observable state. Similarly, the rotational mechanical nature is angular displacement across and torque through a branch.

The associated reference directions of the mechanical terminals correspond directly to the physical directions of displacement and force. As with electrical circuit simulation, a consistent and systematic set of associated reference directions for mechanical terminals is essential. A simple convention specifies translational displacement across variables as positive in the positive-axis directions and the rotational displacement variables as positive in a counterclockwise rotation (right-hand rule) around the positive-axis directions. Through variables going into a branch are interpreted as positive-valued force or torque in the positive direction [60].

Once the terminal natures are defined, the element can be modeled by relating the flow through the terminals to the potential across the terminals. This model is often called a constitutive relationship in network theory. The models need to capture all the physics of the given element, hence a beam element needs to include mass, spring and damping physics, all parametrized by the beam design geometry and the process model parameters. Parametrized models that are within a few percent of continuum simulations have been derived using techniques described in Section 3.

Mechanical parasitics need to be considered for accurate circuit simulation. For example, due to the lumped parameter modeling of the atomic elements, the joint between two beams in a flexure becomes a parasitic. The compliance of the joint is a fringing effect that can be modeled by extending the length of the beams incident at the joint. If one of the beams incident at the joint is significantly wider than the other beam, then the moment relations at the joint need to be considered. Extension factors and the use of plate joints have been verified by comparing the circuit simulation with continuum finite element simulation for all the common flexure topologies and a range of beam sizes. In all cases, the error in flexure compliance and resonant frequency was less than 2%. Additional sources of parasitics include the capacitance and resistances in the interface between the microstructures and electronics.

5.2 Micromechanical Bandpass Filter Circuit

The flexibility of the microelelectromechanical circuit representation is best demonstrated by returning to the bandpass filter example. The filter is composed of three identical resonators, each with a center frequency of 300 kHz, coupled by beam springs [9]. The topology of the filter (Figure 14) with both mechanical structures and interface circuitry is captured in the schematic using the symbols from the NODAS element library [68, 61]. The interface circuitry includes Q-adjustment, frequency tuning, and a trans-resistance sense amplifier.

When an a.c. input voltage, V_{in}, is applied across the electrostatic comb drive, the suspended shuttle masses and flexural beams will be driven by the electrostatic force and move in the x direction. This mechanical vibration is coupled to the other two resonators via the coupling beams, resulting in three resonant peaks, thus forming a passband. The location and spacing of the three peaks are determined by the stiffness of coupling beams, leading to different center frequency and bandwidth. An equivalent SPICE representation is derived in [9, 68] using the methods described in Section 3.2. The equivalent SPICE models represent the mechanical resonators as second-order systems of lumped parameters for mass, spring constant and damping, and represent the coupling beams as massless ideal springs with a coupling spring constant. Figure 15 shows the result of simulating the filter in NODAS with massless beam models compared to the equivalent SPICE model in vacuum. The natural frequency of the resonators is $299.43kHz$, and the quality factor is 495,000. The coupling beams are $88.2\mu m$ long and $1.12\mu m$ wide. There are three peaks around the natural frequency, ranging from $299.43kHz$ to $299.95kHz$. NODAS and SPICE results match to within 4%.

The peaks can be flattened to form a flat passband by applying Q-adjustment series resistors, shown by the simulated filter frequency response in Figure 16. The three sharp peaks of the initial high-Q filter are now compressed down to a nearly flat passband with a ripple of $-21dB$ (Q of 587). NODAS and SPICE simulation results match to within 4%.

The actual flexure and coupling beams have finite mass, and can not be treated as ideal springs, a simplification needed for the analytical derivation of the equivalent SPICE model. Flexure beam mass shifts

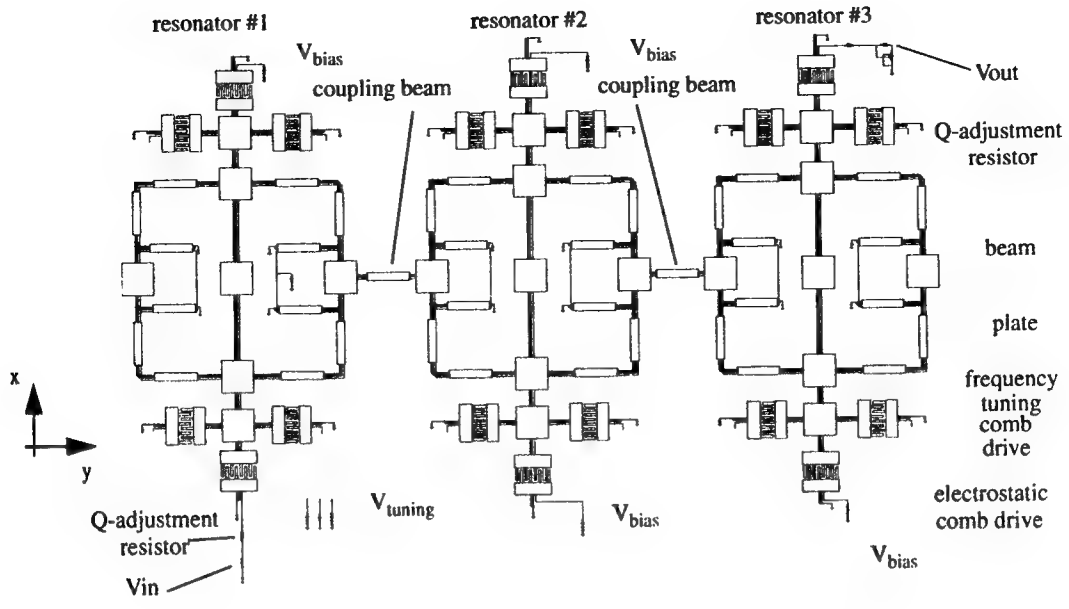

Figure 14: Circuit Schematic of three resonator filter

the center frequency of the filter, while coupling beam mass contributes to the lumped parameter equivalent masses of adjacent resonators also shifts resonant frequencies as well as causes passband distortion. This combined effect can be quantified by comparing the frequency response using the default NODAS beam model (with finite mass) with the response using a massless beam model, as shown in Figure 17.

The combination of ease of schematic entry, simulation accuracy, applicability in iterative design of the wide class of suspended microsystems, compatibility with existing VLSI design flows, and support for co-simulation of electronic and micromachined devices make this micromecahnical circuit simulation approach very attractive. To expand this circuit approach, continued research is needed in identifying the basis elements for enlarged design spaces that include cavitied and hinged structures. Terminal natures for additional physics such as fluidic pressure and flow rate or optical beam intensity are also needed to model new classes of devices. Additionally, methodologies and tools for automated extraction of geometric and material parameters for accurate simulation are crucial for the wide applicability of this simulation-based design approach.

5.3 Extraction from Layout

The circuit-like representation for micromachined devices fits perfectly with the synthesize and optimize phase of device design, as device performance can be simulated but layout details can be avoided. For this representation to be useful during the verification phase, it must be possible, to extract the circuit from the layout. Just like for mainstream integrated circuits, layout extraction involves recognizing patterns in the layout and then inferring a one-to-one correspondence between the layout patterns and the circuit elements.

Layout extraction involves recognition of the layout patterns that correspond to the circuit schematic elements based on their features (shape, size, location). Once the schematic elements are recognized, the extraction creates a connected schematic to capture the shape and location, and annotates the element sizes, thus creating a complete schematic representation of the microstructure layout. The elements can be extracted as fixed values (e.g., plate has $1\mu g$ mass), or as geometrical parameters (e.g., square plate has length of $100\mu m$). The abstractions used for mixed-domain circuit simulation are based on geometrically parametrized models of the atomic elements, requiring extraction of geometrical parameters from the layout. This approach is similar to device extraction in VLSI, where geometrical parameters for the MOS model is extracted from the layout. Unlike VLSI layout extraction, however, the features (shape, size and position) of each layout rectangle is of utmost importance in recognizing the constitutive micromachined atomic elements (VLSI extractors would consider a sequence of beams forming a suspention to be a single wire).

Once the constitutive atomic elements are recognized, element-specific extraction can be used as necessary. This procedure involves purely geometrical reasoning to identify the constitutive schematic elements, followed by determining the appropriate parameters for each instance of an atomic or functional element [63] found

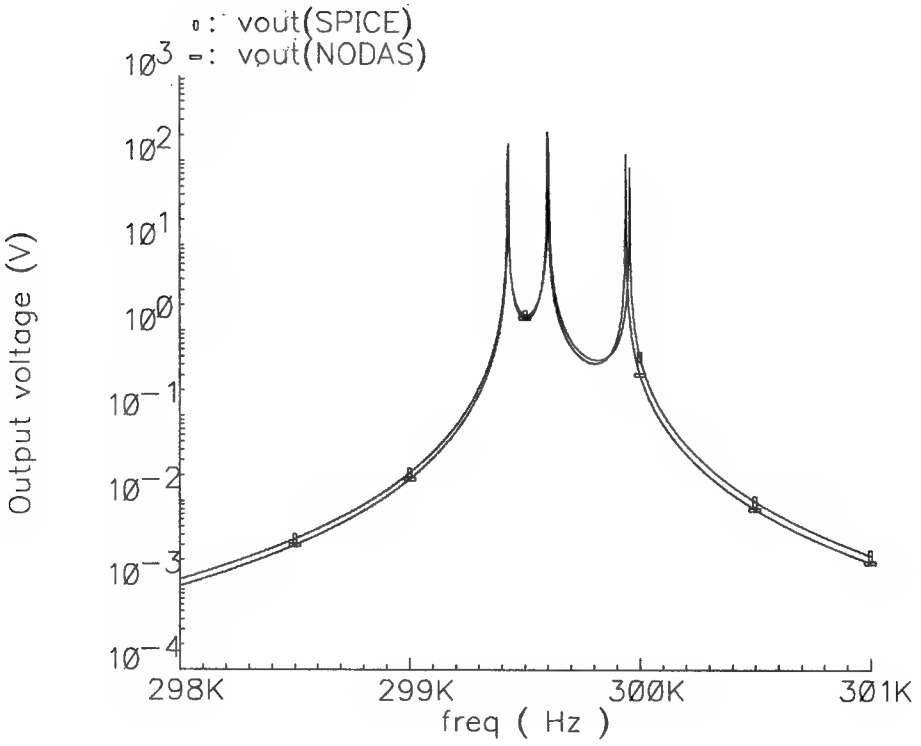

Figure 15: Comparison of NODAS and equivalent SPICE frequency response

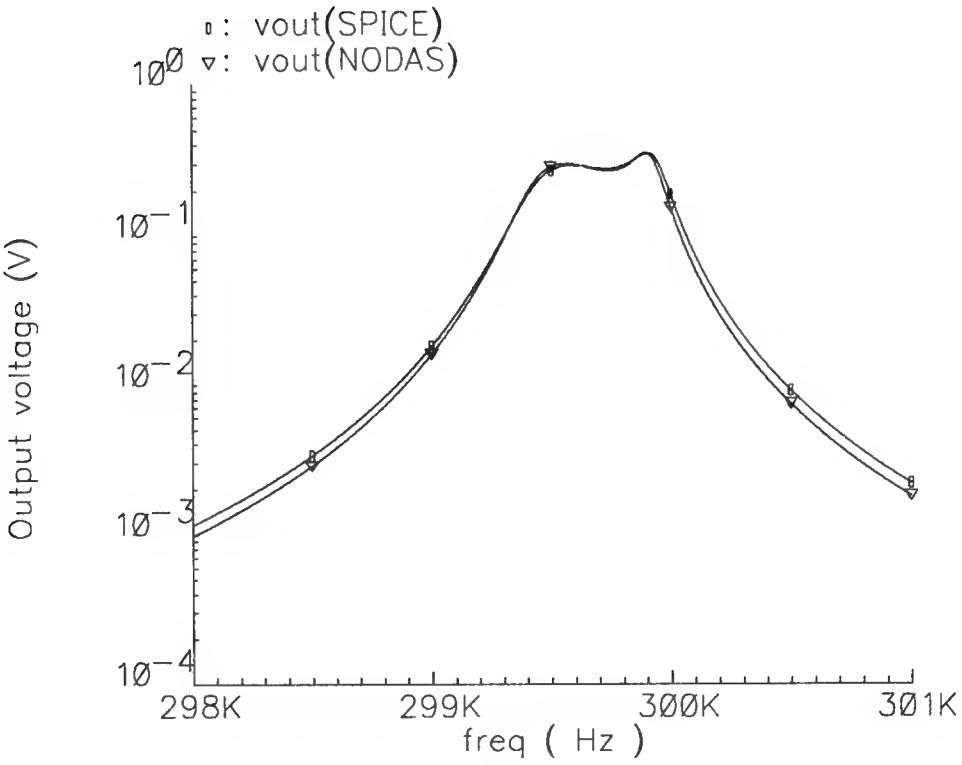

Figure 16: Filter frequency response after Q-adjustment

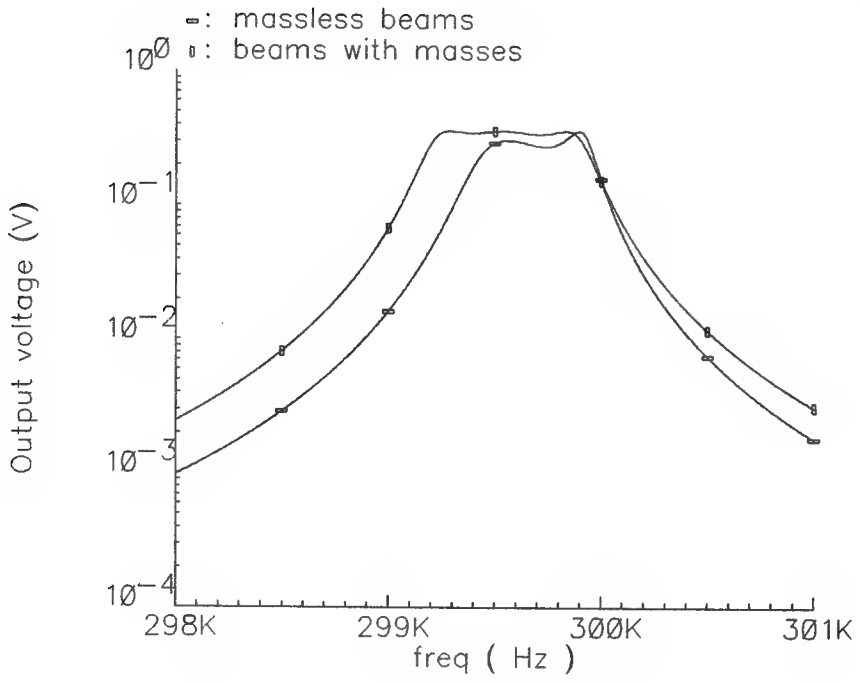

Figure 17: Finite mass effect in frequency response

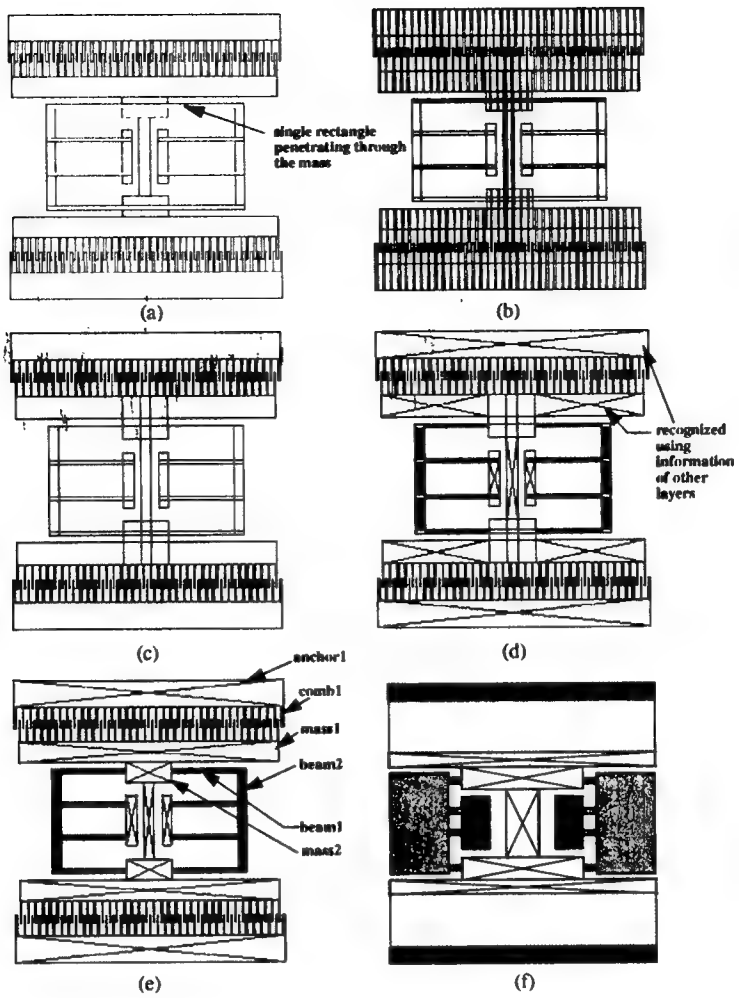

Figure 18: Folded flexure resonator (a) layout, (b) canonical representation, (c) canonical representation after separating the fingers, (d) intermediate state, (e) detected state, (f) functional elements detected

in the layout. In addition to extracting a schematic representation from the layout, parasitics can also be identified and extracted [53, 54].

Rectangles that comprise the layout are generated by algorithms specific to the layout editing tools. The first step in feature recognition for Manhattan-geometry structures therefore involves creating a unique representation of the layout. Starting from an input layout in CIF (Caltech Interchange Form, shown in Figure 18(a)), the rectangles in the layout are partitioned into a canonical representation, such that each rectangle (or cell) has only one neighbor on each side (shown in Figure 18(b)). The use of the canonical representation allows the development of algorithms that are independent of the CAD software used to generate the input layout. The disadvantage of the canonical representation is a significant increase in the number of rectangles to be processed. Most of this increase comes from the presence of fingers in the design, hence they are removed, and the layout re-canonized, as shown in Figure 18(c). The functionality of each of the cells is then determined by its shape, size and connectivity. Non-structural mask layers (such as those that define anchors) are used to obtain hints for possible functional uses for each of the cells, using rules from a process description file. Also contained in this file are rules for atomic element recognition, for example, cells with one connected side are cantilever beam fingers, and cells with connections on opposing sides are considered to be beams. The partitioning due to the canonical representation algorithm results in multiple adjacent cells performing the same function. These multiple cells have to be combined to minimize the number of unnecessary nodes in the netlist. Cell merging, first in the horizontal direction, and then in the vertical direction accomplishes this for the mass and anchor cells. This merging reduces the total number of ports in

the generated netlist, hence contributes to the management of the simulation time for the extracted netlist. The resulting netlist directly corresponds to the atomic elements (beams, plates, gaps and anchors) as shown in Figure 18(e) in the circuit representation of Section 5.1. Thus the primary objective of having a check on the designed layout can be achieved. Device function can also be confirmed via the "circuit" simulation in Section 5.2 on this netlist.

Higher-level functional element models can be detected by processing the extracted netlist. A functional element library containing rules for detecting commonly used spring suspensions and comb-drive topologies is external to the extraction tool, and can be customized to alternate processes and design styles. Finger orientation, region of occurrence, and geometrical parameters (length, width and inter-finger gap) are used to partition the set of recognized fingers, which are then analyzed for connectivity resulting in the extracted comb-drives. Spring detection is accomplished via a finite state machine (FSM) based algorithm. Starting from a start state (always an anchor atomic element), the type of beam and joint determines transitions into the intermediate states, and onto the final state, which indicates the type of spring detected. The joint transitions are classified according to the number of ports and the direction of rotation, and provide the fundamental abstraction on which this FSM-based detection works. The FSM for each of the springs is described in the component library. The connected sets of beams and springs obtained after the atomic recognition is passed through each of these FSMs to recognize their type, as shown by the example in Figure 18(f). Simulation-based verification using this level of extraction is an order of magnitude faster than at the atomic element level, and is seen to be crucial for an iterative design methodology.

The challenge for the extraction methodology is to provide a rich set of basic recognition functions and a language for combining these functions in both process-independent element recognition, and process-dependent use of layer information to support recognition and extraction of all layouts that can be mapped to the circuit element library. This has yet to be demonstrated for non-Manhattan geometry structures in single-structural layer polysilicon micromachining processes. However, for the commonly used Manhattan-geometry suspended microstructure design style and polysilicon micromachining process, extraction has been extremely effective in microstructure layout verification.

6 Conclusions

In this survey paper we presented and contrasted three different approaches for extending circuit simulation to include micromachined devices. The most commonly used method, that of using physical insight to develop parameterized macromodels, is presented first. The issues associated with fitting the parameters to simulation data while incorporating design attribute dependencies was shown to require sophisticated intervention. In addition, the semi-analytic approach did not seem to provide a very effective verification path. Then, the numerical model order reduction approach to macromodeling was presented, and it was shown that the key difficulty remains finding automatic way to perform nonlinear model reduction. In addition, model-order reduction seemed to be ineffective during the synthesis and optimization phase of design, because no attribute sensitivities were computed. Lastly, we described the recently developed circuit-based approach for simulating micromachined devices, and described the design hierarchy and the use of a catalog of parts. We also showed that the circuit-based approach can be combined with extraction from layout, providing an effective approach to verification. The only short-coming of this circuit-based approach is that only some design styles and technology can be supported.

The research effort is sponsored in part by NSF CAREER award MIP-9625471 by the NSF awards MIP-9901171 and CCR-9901195 and by the Defense Advanced Research Projects Agency (DARPA) and Rome Air Force Research Laboratory, Air Force Materiel Command, USAF, under agreements number F30602-96-2-0304 and F30602-97-2-0333.

References

[1] C. Lu, M. Lemkin and B. E. Boser, "A monolithic surface micromachined accelerometer with digital output," *Proc. IEEE Int. Solid-State Circuits Conf.*, San Francisco, CA, Feb. 1995.

[2] P. F. Van Kessel, L. J. Hornbeck, R. E. Meier, and M. R. Douglass, "A MEMS-based Projection Display," IEEE Proceedings, Aug, 1998, pp 1687-1704.

[3] A. V. Chavan and K. D. Wise, "A Monolithic Fully-Integrated ncuum-Sealed CMOS Pressure Sensor," Proc. of 13th IEEE Intl. Conf. on Micro Electro Mechanical Systems (MEMS '00), Miyazaki, Japan, Jan 23-27, 2000, pp. 341-346.

[4] C. T.-C. Nguyen, "MEMS for Wireless Communications", *Proc. IEEE Micro Electro Mechanical Systems Workshop*, Heidelberg, Germany, 1998.

[5] D. J. Harrison and P. G. Glavina, "Towards Miniaturized Electrophoresis and Chemical Analysis Systems on Silicon: An Alternative to Chemical Sensors, Sens. Actuators B 10, 1993

[6] A. H. Epstein et al., "Power MEMS and Microengines," *Sensors and Actuators*, Chicago, IL, June, 1997.

[7] J. Voldman, M. L. Gray, M. A. Schmidt, "Microfabrication in Biology and Medicine," Annu. Rev. Biomed. Engr., 1999, Vol 1.

[8] B. F. Romanowicz, "Methodology for the Modeling and Simulation of Microsystems," Kluwer Academic Publishers, Boston, 1998

[9] K. Wang and C.T.-C. Nguyen, "High-Order Micro-mechanical Electronic Filters," IEEE MEMS Workshop, Nagoya, Japan, January 26-30, 1997, pp.25-30.

[10] P. M. Osterberg and S. D. Senturia, "Membuilder: An automated 3D solid-model construction program for microelectromechanical structures, *Proc. Transducers '95*, Stockholm, Sweden, June 1995

[11] J. M. Funk, J. G. Korvink, J. Buhler, M. Bachtold, and H. Baltes, "SOLIDIS: A Tool for microactuator simulation in 3-D," J. Microelectromech. Syst., vol 6, no 1, 1997

[12] D. Ramaswamy, N. Aluru and J. White, Fast Coupled-Domain, Mixed-Regime Electromechanical Simulation Proc. Int'l Conference on Solid-State Sensors and Actuators (Transducers '99), Sendai Japan, June, 1999 pp. 314-317

[13] S. Crary and Y. Zhang, "CAEMEMS: An Integrated Computer-Aided Engineering Workbench for micro-electro-mechanical systems," *Proc. IEEE Micro Electro Mechanical Systems*, Napa Valley, CA, Feb. 1990.

[14] S. Senturia, "CAD Challenges for Microsensors, Microactuators, and Microsystems," *Proc. IEEE*, vol. 86, August 1998.

[15] Y.-H. Cho, B.-M. Kwak, A. P. Pisano and R. T. Howe, "Viscous energy dissipation in laterally oscillating planar microstructures: a theoretical and experimental study." *Proceedings. IEEE. Micro Electro Mechanical Systems. An Investigation of Micro Structures, Sensors, Actuators, Machines and Systems (Cat. No.93CH3265-6)*. IEEE. pp.93-8. New York, NY, USA, 1993.

[16] W. Ye, X. Wang, and J. White A Fast Stokes Solver for Generalized Flow Problems *International Conference on Modeling and Simulation of Microsystems, Semiconductors, Sensors and Actuators*, San Diego, March 2000

[17] Y. Gianchandani and S. Crary, "Parameteric Modeling of a Microaccelerometer: Comparing I- and D-Optimal Design of Experiments for Finite-Element Analysis," Journal of Microelectromechanical Systems, Vol. 7, No. 2, June 1998.

[18] S. D. Senturia, R. M. Harris, B. P. Johnson, S. Kim, K. Nabors, M. A. Shulman, and J. K. White, "A Computer-Aided Design System for Microelectromechanical Systems (MEMCAD)," *IEEE Journal of Microelectromechanical Systems*, March 1992, Vol. 1, No. 1, p3-13.**

[19] J. R. Gilbert, P. M. Osterberg, R. M. Harris, D. O. Ouma, X. Cai, A. Pfajfer, J. White, and S. D. Senturia, "Implementation of a MEMCAD System for Electrostatic And Mechanical Analysis of Complex Structures From Mask Descriptions," *Proc. IEEE Micro Electro Mech. Syst.*, Fort Lauderdale, February 1993.**

[20] G. M. Koppelman, "OYSTER, a three dimensional structural simulator for microelectromechanical system design," *Sensors and Actuators*, vols. 20, nos. 1/2, 1989

[21] M. Bachtold, J.G. Korvink, H. Baltes, "The Adaptive, Multipole-Accelerated BEM for the Computation of Electrostatic Forces," Proc. CAD for MEMS, Zurich, 1997, pp. 14.

[22] E. J. Grimme, D. C. Sorensen, and P. Van Dooren. Model Reduction of State Space Systems via an Implicitly Restarted Lanczos Method. *Numer. Algorithms*, 1995

[23] Youcef Saad and Martin H. Schultz. GMRES: A generalized minimal residual algorithm for solving nonsymmetric linear systems. *SIAM J. Sci. Statist. Comput.*, 7(3):105–126, 1986.

[24] J. Barnes and P. Hut. A hierarchical $O(N \log N)$ force-calculation algorithm. *Nature*, 324:446–449, 1986.

[25] R. W. Hockney and J. W. Eastwood, *Computer simulation using particles.* New York: Adam Hilger, 1988.

[26] V. Rokhlin, "Rapid solution of integral equation of classical potential theory," *J. Comput. Phys.*, vol. 60, pp. 187–207, 1985.

[27] K. Nabors and J. White, "Fastcap: A multipole accelerated 3-D capacitance extraction program," *IEEE Transactions on Computer-Aided Design of Integrated Circuits and Systems*, vol. 10, pp. 1447–1459, November 1991.

[28] K. Nabors, F. T. Korsmeyer, F. T. Leighton, and J. White. Preconditioned, adaptive, multipole-accelerated iterative methods for three-dimensional first-kind integral equations of potential theory. *SIAM J. Sci. Statist. Comput.*, 15(3):713–735, 1994.

[29] J. R. Phillips and J. K. White, "A Precorrected-FFT method for Electrostatic Analysis of Complicated 3-D Structures," *IEEE Trans. on Computer-Aided Design*, October 1997, Vol. 16, No. 10, pp. 1059-1072.

[30] D. Ramaswamy, N. Aluru and J. White, Fast Coupled-Domain, Mixed-Regime Electromechanical Simulation Proc. Int'l Conference on Solid-State Sensors and Actuators (Transducers '99), Sendai Japan, June, 1999 pp. 314-317

[31] L. Greengard, V. Rokhlin, "A New Version of the Fast Multipole Method for the Laplace Equation in Three Dimensions," Acta Numerica, 1997, pp. 229-269.

[32] W. Hackbusch and Z. P. Nowak, "On the Fast Matrix Multiplication in the Boundary Element Method by Panel Clustering," Numer. Math. 54, pp. 463-491, 1989.

[33] K.J. Bathe, Finite Element Procedures, Prentice-Hall Inc., Englewood Cliffs, NJ,1996.

[34] N.R. Aluru and J. White, "A Coupled Numerical Technique for Self-Consistent Analysis of Micro-Electro-Mechanical Systems", Microelectromechanical Systems (MEMS), ASME Dynamic Systems and Control (DSC) series, New York, Vol. 59, pp.275-280,1996.

[35] E. Huang, Y. Yang, and S. Senturia, "Low-Order Models For Fast Dynamical Simulation of MEMS Microstructures," IEEE Int. Conf. on Solid State Sensors and Actuators(Transducers '97), Chicago, June 1997, Vol. 2, pp. 1101-1104.

[36] M. Varghese, V. Rabinovich, M. Kamon, J. White. S. Senturia, "Reduced-Order modeling of Lorentz force actuation with Mode Shapes," International Conference on Modeling and Simulation of Microsystems, Semiconductors, Sensors and Actuators, San Juan, April 1999

[37] J. Phillips, "Automated Extraction of Nonlinear Circuit Macromodels," Cadence technical report, December, 1999.

[38] E. S. Hung, Y. J. Yang and S. D. Senturia. Low-Order models for fast dynamical simulation of MEMS microstructure. *IEEE International Conference on Solid-State Sensors and Actuators (Transducers '97)*, 4(A2.03):1101–1104, June 1997.

[39] P. Feldmann and R. W. Freund. Efficient Linear Circuit Analysis by Padé Approximation via the Lanczos Process. *IEEE Trans. Computer-Aided Design*, Vol. 14, No.5, pp.639-649, May 1995

[40] A. Odabasioglu, M. Celik, and L. Pileggi. PRIMA: Passive Reduced-Order Interconnect Macromodeling Algorithm. *IEEE Conference on Computer-Aided Design*, San Jose, CA, 1997

[41] K. Glover. All Optimal Hankel-norm Approximations of Linear Multivariable Systems and Their L^∞-error Bounds. *Int. J. Control*, Vol.39, No.6, pp.1115-1193, 1984

[42] Y. Chen and J. White "A Quadratic Method for Nonlinear Model Order Reduction," International Conference on Modeling and Simulation of Microsystems, Semiconductors, Sensors and Actuators, San Diego, March 2000.

[43] J. Chen and S. Kang "Techniques for Coupled Circuit and Micromechanical Simulation," International Conference on Modeling and Simulation of Microsystems, Semiconductors, Sensors and Actuators, San Diego, March 2000.

[44] Yong Chen, Model Order Reduction for Nonlinear Systems, MIT MS thesis, September 1999

[45] L. Gabbay, J. Mehner and S. Senturia, "Computer-Aided Generation of Nonlinear Reduced-Order Dynamic Macromodels: I. Non-Stress-Stiffened Case,", to appear, J. Microelectromechanical Systems.

[46] E.K. Antonsson, "Structured Design Methods for MEMS," NSF Sponsored Workshop on Structured Design Methods for MEMS, November 12-15, 1995.

[47] N. R. L. Lo, E. C. Berg, S. R. Quakkelaar, J. N. Simon, M. Tachiki, H.-J. Lee, and K. S. J. Pister, "Parametrized Layout Synthesis, Extraction, and SPICE Simulation for MEMS," Proc. 1996 IEEE Intl. Symp. on Circuits and Systems, Atlanta, GA, May 12-15, 1996, pp 481-484.

[48] J. M. Karam, B. Courtois, H. Boutamine, P. Drake, A. Poppe, V. Szekely, M. Rencz, K. Hofmann and M. Glesner, "CAD and foundries for microsystems," Proc. 34th Design Automation Conference (DAC '97), Anaheim, CA, June 9-13, 1997, pp. 674-679.

[49] T. Mukherjee and G. K. Fedder, "Structured Design of Microelectromechanical Systems," in Proc. 34th Design Automation Conference (DAC '97), Anaheim, CA, June 1997, pp. 680-685.

[50] G. K. Fedder, "Structured design for Integrated MEMS," IEEE MEMS '99, Orlando, FL, January 17-21, 1999, pp. 1-8.

[51] T. Mukherjee, G. K. Fedder and R. D. Blanton, "Hierarchical Design and Test of Integrated Microsystems," IEEE Design and Test, vol. 16, no. 4, Oct-Dec 1999, pp. 18-27.

[52] N. Swart, "A Design Flow for Micromachined Electromechanical Systems," IEEE Design and Test, vol. 16, no. 4, Oct-Dec 1999, pp. 39-47.

[53] G. K. Fedder, "Top-Down Design of MEMS," Proc. 2000 Intl. Conf. on Modeling and Simulation of Microsystems (MSM 2000), San Diego CA, March 27-29, 2000.

[54] T. Mukherjee, "CAD for Integrated MEMS Design," Proc. Design, Test Integration, and Packaging of MEMS/MOEMS (DTIP 2000), Paris, France, May 9-11, 2000.

[55] ADXL202 Accelerometer Data Sheet, Analog Devices, Inc., One Technology Way, P.O.Box 9106, Norwood, MA 02062-9106, 1998 (http://www.analog.com).

[56] J. E. Vandemeer, M. S. Kranz, and G. K. Fedder, "Nodal Simulation of Suspended MEMS with Multiple Degrees of Freedom," Proc. 1997 International Mechanical Engineering Congress and Exposition: The Winter Annual Meeting of ASME in the 8th Symposium on Microelectromechanical Systems, Dallas, TX, Nov. 16-21, 1997

[57] J. E. Vandemeer, M. S. Kranz, G. K. Fedder, "Hierarchical Representation and Simulation of Micromachined Inertial Sensors," Proc. 1998 Int. Conf. on Modeling and Simulation of Microsystems, Semiconductors, Sensors and Actuators (MSM '98), Santa Clara, CA, April 6-8, 1998.

[58] G. Lorenz and R. Neul, "Network-Type Modeling of Micromachined Sensor Systems," Proc. 1998 Int. Conf. on Modeling and Simulation of Microsystems, Semiconductors, Sensors and Actuators (MSM '98), Santa Clara, CA, April 6-8, 1998.

[59] G. K. Fedder and Q. Jing, "NODAS 1.3 - Nodal Design Of Actuators And Sensors," in Proc. of IEEE/VIUF Int. Workshop on Behavioral Modeling and Simulation, Orlando, FL, October 27-28, 1998.

[60] G. K Fedder and Q. Jing, "A Hierarchical Circuit-level Design Methodology for Microelectromechanical Systems," IEEE Trans. on Circuits and Systems-II, vol. 46, no. 10, Oct. 1999, pp. 1309-1315.

[61] Q. Jing, H. Luo, T. Mukherjee, L. R. Carley, and G. K. Fedder, "CMOS Micromechanical Bandpass Filter Design Using a Hierarchical MEMS Circuit Library," Proceedings of Thirteenth IEEE International Conference on Micro Electro Mechanical Systems (MEMS '00), Miyazaki, Japan, pp. 187-192, January 23-27, 2000.

[62] B. Baidya, S. K. Gupta, and T. Mukherjee, "Feature-recognition for MEMS Extraction," in CDROM Proc. of 1998 ASME DETC Design Automation Conferences, Atlanta, GA, September 13-16 1998.

[63] B. Baidya, S. K. Gupta and T. Mukherjee, "MEMS Component Extraction," in Proc. 1999 Intl. Conf. on Modeling and Simulation of Microsystems (MSM '99), San Juan Puerto Rico, April 19-21 1999, pp. 143-146.

[64] J. Clark, N. Zhou, S. Brown and K.S.J. Pister, "Nodal Analysis for MEMS Simulation and Design," Proc. 1998 Intl. Conf. on Modeling and Simulation of Microsystems (MSM 98), Santa Clara, CA, April 6-8, 1998.

[65] J. Clark, N. Zhou, S. Brown, and K.S.J.Pister, "Fast, accurate MEMS simulation with SUGAR 0.4," Proc. of the Sensors and Actuator Workshop, Hilton Head Is., SC, June 1998.

[66] J. Clark, N. Zhou, and K.S.J.Pister, "Modified Nodal Analysis for MEMS with Multi-Energy Domains" Proc. 2000 Intl. Conf. on Modeling and Simulation of Microsystems (MSM 2000), San Diego CA, March 27-29, 2000.

[67] D. Teegarden, G. Lorenz and R. Neul, "How to model and simulate microgyroscope systems," IEEE Spectrum, Vol 35, No. 7, pp. 66, 1998.

[68] Q. Jing, T. Mukherjee, and G. K. Fedder, "A Design Methodology for Micromechanical Bandpass Filters," in Proc. 1999 IEEE/ACM Intl. Workshop on Behavioral Modeling and Simulation (BMAS 99), Orlando, Florida, October 4-6, 1999.

*U.S. GOVERNMENT PRINTING OFFICE: 2000-610-055-10027

DISTRIBUTION LIST

addresses	number of copies
ROBERT G. HILLMAN AFRL/IFTC 26 ELECTRONICS PKWY ROME NY 13441-4514	10
DR. GARY K. FEDDER CARNEGIE MELLON UNIVERSITY 5000 FORBES AVE PO BOX 371032M PITTSBURG PA 15213-3890	2
AFRL/IFOIL TECHNICAL LIBRARY 26 ELECTRONIC PKY ROME NY 13441-4514	1
ATTENTION: DTIC-OCC DEFENSE TECHNICAL INFO CENTER 8725 JOHN J. KINGMAN ROAD, STE 0944 FT. BELVOIR, VA 22060-6218	1
DEFENSE ADVANCED RESEARCH PROJECTS AGENCY 3701 NORTH FAIRFAX DRIVE ARLINGTON VA 22203-1714	1
DR ANANTHA KRISHNAN DARPA/MTO 3701 N FAIRFAX DRIVE ARLINGTON VA 22203	5

MISSION
OF
AFRL/INFORMATION DIRECTORATE (IF)

The advancement and application of Information Systems Science and Technology to meet Air Force unique requirements for Information Dominance and its transition to aerospace systems to meet Air Force needs.